Title

PRODUCTION AND DECAY PROPERTIES OF THORIUM ISOTOPES OF MASS 221-224 FORMED IN HEAVY ION REACTIONS

Authors

Valli, Kalevi
Hyde, Earl K.
Borggreen, Jorn.

Publication Date

1969-10-01

Submitted to Physical Review

UCRL-18992
Preprint

c. 2

PRODUCTION AND DECAY PROPERTIES OF THORIUM ISOTOPES OF MASS 221-224 FORMED IN HEAVY ION REACTIONS

Kalevi Valli, Earl K. Hyde, and Jørn Borggreen

October 1969

AEC Contract No. W-7405-eng-48

LAWRENCE RADIATION LABORATORY
UNIVERSITY of CALIFORNIA BERKELEY

DISCLAIMER

PRODUCTION AND DECAY PROPERTIES OF THORIUM ISOTOPES OF MASS 221-224 FORMED IN HEAVY ION REACTIONS

Kalevi Valli,† Earl K. Hyde, and Jørn Borggreen‡

Nuclear Chemistry Division
Lawrence Radiation Laboratory
University of California
Berkeley, California

October, 1969

ABSTRACT

In order to search for new neutron-deficient isotopes of uranium and thorium, targets of ^{209}Bi and ^{208}Pb were bombarded with beams of ^{22}Ne, ^{20}Ne, ^{19}F, ^{18}O, ^{16}O, ^{14}N, and ^{12}C in the Berkeley HILAC. The reaction products were transported from the reaction cell by the helium jet technique and their alpha disintegration characteristics measured by on-line techniques of alpha spectroscopy. Energy values, excitation functions, and half lives of alpha particle groups were measured. Only fragmentary evidence for uranium nuclei was found because of intense losses by nuclear fission but definite proof was obtained for the previously-unknown millisecond isotopes ^{222}Th and ^{221}Th and for their decay products ^{218}Ra, ^{214}Rn, ^{217}Ra, and ^{213}Rn. Improvements were made on the literature values for ^{223}Th and its decay products.

The new alpha data help greatly in the determination of the trends in alpha decay energies for isotopes of even Z elements particularly in the poorly defined region just above the 126 neutron shell. This allows the preparation of more reliable set of predictions for many unknown nuclei.

---

*This work was performed under the auspices of the U.S. Atomic Energy Commission

†Present address, Dept. of Physics, University of Helsinki, Helsinki, Finland

‡On leave from Niels Bohr Institute, Risø, Denmark

I. INTRODUCTION

We have published a series of papers on the alpha-decay properties of neutron-deficient isotopes of astatine,[1] radon,[2] francium,[3] radium,[4] actinium,[5] and thorium.[6] In this work heavy element targets were bombarded at the Berkeley Heavy Ion Linear Accelerator (HILAC) with beams of ^{12}C, ^{14}N, ^{16}O, ^{20}Ne and other ions. The helium-jet transfer technique was employed to transport the products of the nuclear reaction from the gas-filled reaction cell into an evacuated counting chamber where the alpha radiations of those products could be studied with semiconductor detectors. Half-lives of the nuclides reported in these studies fell in the range of minutes down to milliseconds.

The purpose of the present research was to exploit the improved speed capabilities of the helium-jet transfer technique[6] in order to get information on an island of "missing" nuclides with neutron number 128 or a few greater and atomic number between 86 (radon) and 92 (uranium) (see Fig. 1). The present lack of information on these neutron-deficient nuclei is caused by the difficulty in preparing them and by their short alpha-decay lifetimes which reflect the high alpha-decay energies for nuclides just beyond the 126-neutron shell. The general plan was to prepare isotopes of uranium and thorium with mass numbers less than those previously reported. Several of these could be expected to have half-lives within the millisecond range of the on-line techniques and furthermore, they could be expected to initiate a chain of alpha decays which would provide information on radium and radon daughter activities. These daughter products could not be studied as direct reaction products owing to their microsecond half-lives.

This new information was sought partly for the intrinsic interest in nuclear data on unknown nuclei and partly for the importance of the alpha decay data in mapping out the systematic trends in alpha decay energies near the 126 neutron shell. This information in turn has considerable importance for the estimation of ground state masses, the evaluation of atomic mass formulas, etc.

An additional strong reason for this study is the need for the results in a proper interpretation of alpha data observed in the interaction of heavy-ion projectiles with uranium or transuranium element targets when these interactions are studied with the goal to produce new isotopes of transfermium elements. Inasmuch as the alpha decay energies and half lives of some of these isotopes may be similar to those of the nuclides in the lead to uranium region and inasmuch as the lighter products may be produced by unusual nuclear breakup or transfer reactions in the heavy target or by reactions induced in lead or bismuth trace impurities in the target, it is quite important that the properties of these lighter nuclides be well known.

Targets of ^{209}Bi, ^{206}Pb, ^{208}Pb, and ^{205}Tl were bombarded with beams of ^{22}Ne, ^{20}Ne, ^{19}F, ^{18}O, ^{16}O, ^{14}N, ^{12}C, and ^{11}B in order to produce excited compound nuclei of uranium, protactinium, thorium, actinium, radium, and radon. Eighteen combinations of target and projectile including those listed in Table I were studied but the main results were obtained with the combinations $^{208}Pb + ^{22}Ne$, $^{208}Pb + ^{20}Ne$, $^{209}Bi + ^{19}F$, and $^{208}Pb + ^{16}O$. In this regard the ^{22}Ne beam capability of the HILAC was particularly valuable.

For each reaction system the radiations emitted by the collected reaction products were measured with semiconductor detectors to determine the

alpha energy spectrum, the relative abundances, and the half lives of the peaks in the spectrum. From these data and from the changes in the spectra as a function of the bombarding energy, it was possible to determine the nuclide responsible for nearly every peak in the spectra and to establish genetic relationships. These assignments were strengthened by arguments based on the energetics of the nuclear reactions and on the expected trends in alpha-decay properties.

The main advantages of our experimental techniques are that the lightest isotopes of the elements of interest are prepared free of contamination with heavier isotopes and are isolated rapidly without the necessity for radiochemical separation techniques, so that products with half-lives as short as milliseconds can be investigated. The lightest isotopes of uranium in published reports[7,8] are 58 minute ^{229}U, 9.1 minute ^{228}U, and 1.3 minute ^{227}U prepared by $(\alpha,7n)$, $(\alpha,8n)$, and $(\alpha,9n)$ reactions, respectively, on ^{232}Th targets. Uranium-227 has also been made by the $^{234}Pa(p,5n)^{227}U$ reaction.[9] The lightest thorium isotopes known from past work[7] (with the exception of the mass 213-217 group studies in our own work[6]) are 0.9 second ^{223}Th, 1 second ^{224}Th, and 8.0 minute ^{225}Th. These have been studied as members of decay chains supported by decay of longer-lived uranium parents.

Although the heavy-ion reaction method has some strong advantages over the (α,xn) method for the stated purposes, it has the big disadvantage that the yields of the products of compound nucleus reactions are more severely reduced by nuclear fission, probably because of the high angular momentum brought into the compound nucleus by the heavy projectile. At a bombarding energy sufficient to overcome the high Coulomb barrier, the excitation of the nucleus is adequate for the evaporation of three or four neutrons and at each

evaporation step there is a loss by fission competition; at the high bombarding energies the loss via nuclear fission is progressively greater. As a result we were not able to prepare samples of the uranium isotopes. On the other hand the fission competition in reactions of the type (projectile, α xn) was much less and consequently the yield of the "alpha out" product was considerably enhanced relative to the pure neutron evaporation product so that the dominant contribution to the alpha spectra came from the reactions of "alpha-out" type. Thus, in the bombardment of ^{208}Pb with neon isotopes the yield of thorium isotopes was moderately high. There was also some lesser contribution to the observed products from "proton-out" reactions such as the following examples: $^{208}Pb(^{16}O,pxn)^{223-x}Ac$ and $^{209}Bi(^{16}O,pxn)^{224-x}Th$.

Figure 1 shows the four series of genetically-related nuclides about which new information was obtained in this study and shows their location in the chart of the nuclides. The stable isotopes used as targets are also shown in the figure.

Another consequence of the removal of the main reaction products by nuclear fission is the prominence in the alpha spectra of peaks from another group of products resulting from transfer of a few nucleons from the projectile to the target. The most prominent of these are ^{211}Po, ^{211m}Po, and ^{212}At and ^{212m}At made by the transfer of a few protons and neutrons to the ^{208}Pb or ^{209}Bi targets. In some experiments ^{214}Fr and ^{214m}Fr were also produced. These partial transfer reactions are quite interesting in themselves and warrant further study, but in the present investigation they provided unwanted background.

As Fig. 1 indicates, the results in this paper relate only to even Z products in the group of nuclei with more than 127 neutrons. In a second

paper[10] we shall discuss our results on alpha-decay chains initiated by neutron deficient isotopes of protactinium in which new information is presented on isotopes of protactinium, actinium, and francium.

The experimental techniques are described in the following section and the results on individual chains of alpha emitters are presented in the succeeding sections.

II. EXPERIMENTAL

The experimental techniques were the same as those described in detail in a previous report[6] so we present only the essential features here. The apparatus consisted of a 1 cm^3 target chamber kept filled with helium to a pressure of two atmospheres and of an adjacent large counting chamber evacuated continuously with a vacuum pump of high capacity. A capillary 8 cm long and 0.5 mm in diameter connected the two chambers. The heavy ion beam entered the target chamber through a window of thin nickel foil, passed through a thin layer of the target material deposited on the back surface of the nickel window, emerged from the reaction cell through another thin nickel window, and finally stopped in a Faraday cup. Nuclear reaction products recoiling out of the target were slowed down by collisions with the helium gas atoms and became entrapped in the stream of helium sucked out of the reaction cell through the capillary into the evacuated counting chamber. The gas jet impinged on a metallic surface and the heavy recoil atoms, traveling at near-sonic velocity, stuck to this surface.

The alpha decay of the collected nuclei was detected by a semiconductor detector facing the collector. The signals from the detector were amplified

by standard electronic techniques and the amplitudes of the final pulses were measured with a 1024-channel analog-to-digital converter coupled to a PDP-7 computer. A special electronic programmer was used to synchronize data collection and storage with the operation of the accelerator. The normal duration of the HILAC beam pulses was 4 msec with 20 msec between pulses. In the usual mode of data collection the computer input was blocked during the beam bursts when the radiation background was high and was gated on during the interval between successive beam pulses.

In normal operation the energy of the HILAC beam was fixed at 10.3 MeV per nucleon. Thus the maximum energies of the ions used in this study were ^{22}Ne 227 MeV, ^{20}Ne 206 MeV, ^{19}F 196 MeV, ^{16}O 165 MeV, ^{18}O 185 MeV, ^{14}N 144 MeV, ^{12}C 124 MeV, and ^{11}B 113 MeV. Lower beam energies were obtained by inserting stacks of 1.72 mg/cm^2 aluminum foils by means of an absorber wheel placed in front of the entry window of the reaction cell. The range-energy relationships of Northcliffe[11,12] were used to calculate the beam energy degradation in the absorber foils, in the chamber window, and in the target material.

For the purpose of making quantitative measurements of the changes in the spectra with change in beam energy, the beam was measured with a Faraday cup and series of measurements were made with different values of beam energy for a standardized value of the integrated beam current. A typical run time for an individual measurement was 30-60 minutes at a beam current of 200-500 nanoamperes.

For the purpose of making half-life measurements the electronic programmer was used in other modes of operation. For half-lives in the millisecond range the period between beam bursts was divided into 4, 8, or 16 equal intervals

and the alpha disintegrations occurring in each time period were recorded in different sections of the computer memory. In the case of longer half-lives the computer input was blocked during a bombardment period equal to several half-lives, after which the beam was turned off and alpha-count data were collected during 4, 8, or 16 equal time periods and separately stored in the computer memory. The beam was then turned back on and the process repeated.

The apparent half-lives determined for activities in the millisecond range had to be corrected for the effect of the 17 millisecond period required to replace one chamber volume of helium as this gas streamed through the chamber.

The targets were prepared in the following manner. The natural bismuth target was made by vacuum evaporation of the element to a thickness of 1.7 mg/cm^2 on nickel or copper foil backing. Separated ^{208}Pb, ^{206}Pb, and ^{205}Tl were obtained from Oak Ridge National Laboratory with the following isotopic compositions: ^{208}Pb 99.3%, ^{207}Pb 0.52%, and ^{206}Pb 0.19%, ^{208}Pb 1.4%, ^{207}Pb 1.3%, and ^{206}Pb 97.2%; and ^{205}Tl 99.0% and ^{203}Tl 1.0%. The thallium targets were vacuum evaporated. Some of the lead targets were vacuum evaporated and others were electroplated. Target thickness varied between 0.5 and 10 mg/cm^2. The most usual thickness was 2-3 mg/cm^2 which is approximately equal to the range of the recoil atoms in the target.

The alpha detectors were silicon surface-barrier detectors with an active area of 50 mm^2 and a 1 mm-diameter hole in the center through which the capillary passed. The distance from the collector surface to the detector corresponded to a solid angle of 15% of 4π. The energy scales for the alpha spectra were determined primarily by use of calibration standards taken from the actinium and thorium series,[13] in particular, ^{211}Bi 6.622 MeV, ^{219}Rn 6.8176 MeV,

^{215}Po 7.3841 MeV, and ^{212}Po 8.7854 MeV. The calibration spectra were measured simultaneously with the reaction spectra to be calibrated in order to eliminate any possibility of gain shifts caused by beam-on and beam-off effects. Some known peaks in the reaction spectra were used as secondary alpha standards, particularly the following: ^{214}Ra 7.136 MeV,[4] ^{215}Ra 8.698 MeV,[6] ^{213}Fr 6.773 MeV,[3] ^{214}Fr 8.426 MeV,[6] and ^{214m}Fr 8.549 MeV.[6]

A general comment should be made on the relative intensities of alpha groups belonging to the same decay chain. The members of the chain with half-lives short compared with the duration of the measurements (~30 min.) reached radioactive equilibrium with each other and thus had equal intensities. This criterion was used in several cases to seek out less prominent groups in the alpha complex structure. However, there are two experimental effects which can distort the intensity pattern. The 25 μsec deadtime of the analog-to-digital converter may depress the intensity of a short-lived daughter by an amount which can be as great as the solid angle of the sample-detector geometry, in our case ~15 percent. Also when the daughter half-life is shorter than the 2 μsec integration time used for pulse shaping in the main amplifier, the pulses from the parent and daughter may pile up causing loss of intensity in both peaks.

A consideration of these effects caused us to devise a method for the measurement of microsecond half-lives. The method makes use of a time-to-amplitude converter (TAC) incorporated in the electronic system shown in Fig. 2. One unconventional feature is the use of signals from the same detector as input to both start and stop sides of the TAC. To prevent an individual pulse from serving simultaneously as start and stop, a delay was inserted on the start side. Any pulse on the start input could fire the TAC for its preset cycle

time and any second pulse reaching the stop input during this cycle time could cause the appearance of a pulse on the time output of the TAC. This time pulse was passed to a computer interface unit. The valid-start and valid-stop output signals were used to gate the passage of the linear signals associated with the start and stop pulses to the same computer interface. The pulse stretching and gating circuitry shown in Fig. 2 was required to insure time coincidence of the three pulses presented to the computer interface.

A computer program, MULTID, was used to control the acceptance and processing of the pulses by a PDP-7 computer. Whenever signals appeared simultaneously on the three inputs the pulse amplitudes were coded and stored as an event record on magnetic tape. The distributions over the three parameters were shown on-line during data recording. After the experiment the events on the magnetic tape record were analyzed with the program MULTIS by setting selection criteria (windows) on any two of the three parameters and examining the corresponding distribution of the third. For example, windows could be set on specific alpha peaks in the start (parent) and stop (daughter) spectra and the corresponding time spectrum examined to determine the half-life of a specific nuclide. In a second sort windows could be set to permit examination of the entire start spectrum corresponding to specific regions of the stop and time spectrum.

The observed effect is proportional to the square of the detection geometry. To increase the latter the alpha activity was collected on the gold surface of a planar semiconductor detector. To permit examination of half-lives as short as 1 μsec time constants of 0.2 μsec were used in the pulse shaping network of the main amplifier.

We owe thanks to Professor R. D. Macfarlane for calling our attention to the usefulness of a TAC unit for such applications.

III. RESULTS

A. The Uranium-228 Decay Chain

Samples of ^{228}U have been isolated previously by Meinke, Ghiorso, and Seaborg,[7] by Orth[14] and by Ruiz[8] from thorium targets bombarded with high energy protons, and the decay chain has been determined to be the following:

$$\underset{9.1\ \text{min}}{^{228}U} \xrightarrow{\alpha} \underset{1.0\ \text{sec}}{^{224}Th} \xrightarrow{\alpha} \underset{23\ \text{msec}}{^{220}Ra} \xrightarrow{\alpha} \underset{45\ \mu\text{sec}}{^{216}Rn} \xrightarrow{\alpha} \underset{0.30\ \mu\text{sec}}{^{212}Po} \xrightarrow{\alpha} \underset{\text{stable}}{^{208}Pb}$$

Within error limits the three investigations agree about the energies of the main alpha groups, as shown in Table II, but the study of Ruiz is the latest and the most complete. Ruiz reported an upper limit of 5% for the electron capture branching of ^{228}U and 100% for the alpha branching of the remaining members of the chain.

In our work none of the available combinations of projectile and target permitted the production of ^{228}U by compound nucleus or partial transfer reactions (see Table I); in the $^{208}Pb + ^{22}Ne$ combination the ^{230}U compound nucleus had too much energy for the emission of only two neutrons and in the $^{209}Bi + ^{22}Ne$ combination the $(^{22}Ne,p2n)$ reaction cross section was low. Hence, it was possible to study the series only from ^{224}Th and the most useful reaction for this proved to be $^{208}Pb(^{22}Ne,\alpha 2n)^{224}Th$.

The alpha groups of ^{224}Th and its daughters produced in this way at two energies of the ^{22}Ne beam are displayed in Fig. 3. Our alpha energies (Table II) agree with those of Ruiz[8] and our value of 1.03 ± 0.05 sec for the half-life of ^{224}Th confirms the value reported by Tove.[15] The excitation curves for the activities were determined by bombarding at several energies for a measured amount of beam current and integrating under each alpha peak in the spectrum (see Fig. 4). With the exception of the complex 7.45 MeV peak the excitation curves have similar shape with yield maxima occuring at 97 MeV beam energy not far above the estimated Coulomb barrier. This is reasonable for the maximum yield of the $^{208}Pb(^{22}Ne,\alpha 2n)$ reaction as judged from our previous studies of reactions of the "alpha-out" type.[5]

The high intensity of the ^{220}Ra peak is due to an admixture of the 7.448 MeV group of ^{211}Po which is produced directly by a partial transfer reaction.

Our results on the ^{224}Th and the remaining members of the chain are summarized in Table II. They confirm what was known previously and are chiefly useful in establishing the validity of the experimental technique and in fixing the excitation energy for the maximum production of a thorium isotope of known mass number. This last information was needed as a check point for the identification of the lighter thorium isotopes produced at higher beam energies.

B. The Uranium-227 Decay Chain

Some preliminary results on the properties of the ^{227}U chain were

obtained by Meinke, Ghiorso, and Seaborg[7] on uranium samples quickly isolated from thorium salts bombarded with 150 MeV helium ions. They formulated the chain as follows:

$$^{227}\underset{1.3\ \text{min}}{U} \xrightarrow{\alpha} {}^{223}\underset{\text{short}}{Th} \xrightarrow{\alpha} {}^{219}\underset{\text{short}}{Ra} \xrightarrow{\alpha} {}^{215}\underset{\text{short}}{Rn} \xrightarrow{\alpha} {}^{211}\underset{0.52\ \text{sec}}{Po} \xrightarrow{\alpha} {}^{207}\underset{\text{stable}}{Pb}$$

These assignments have recently been confirmed by Hahn et al.[9] who prepared the same series by the $^{231}Pa(p,5n)^{237}U$ reaction, except that they obtained somewhat different alpha particle energies (see Table III).

In our work the $^{208}Pb + {}^{22}Ne$ target-projectile combination was the only one possible for the production of ^{227}U by a compound nucleus reaction (Table I): $^{208}Pb(^{22}Ne,3n)^{227}U$. This reaction has its highest yield at a beam energy just above the Coulomb barrier (about 90 MeV), but the ^{227}U yield is greatly reduced by fission and the main contribution to the decay chain comes from ^{223}Th produced directly in the $^{208}Pb(^{22}Ne,\alpha 3n)^{223}Th$ reaction. This reaction has its maximum yield at the higher beam energy of 110 MeV.

In the alpha spectra shown in Fig. 3 there are several peaks which can be assigned to ^{223}Th and to its decay products. In Fig. 4 the yield-versus-bombarding energy curves are shown for several of these peaks. Despite the fact that some of the groups at 7.28, 7.31, 7.68, 7.98, and 8.68 MeV are complex the similarity of the excitation functions indicates that the groups--or significant fractions of them--belong to the same decay chain. This conclusion is supported by the half-life measurements which showed a prominent 0.66 sec component in each of the above energy groups. We show below that the 0.66 sec half-life can be assigned to ^{223}Th which means that the direct

production of ^{223}Th dominates over the indirect production from ^{227}U decay. Hence, we can compare the energy of the peak yield for ^{223}Th (109 MeV) with that for ^{224}Th (99 MeV); the 10 MeV difference is reasonable if the effect of the Coulomb barrier on the ^{224}Th cross section curve is taken into account.

The assignment of the individual peaks to the members of the ^{223}Th decay chain was made on the basis of alpha-particle energies expected from systematic trends in alpha-decay energies and from intensity balance arguments. The resulting assignments are summarized in Table III together with the results of Hahn et al.[9]

The detailed arguments leading to our assignments are presented in the next several paragraphs.

1. Thorium-223

In the $^{208}Pb + ^{22}Ne$ experiments peaks appeared at 7.28 and 7.32 MeV in the spectra (see Fig. 3) with a yield maximum at a bombarding energy of 109 MeV (see Fig. 4). These peaks had a half-life of 0.66 seconds. These properties are reasonable for ^{223}Th except that the 7.31 MeV group is about 300 keV lower than the expected value for the ground state transition (see Fig. 17) so that a weak ground state transition of 7.65 MeV may remain to be found. This would not be surprising since the favored decay for ^{225}Th, ^{227}Th, and ^{229}Th is to a level 200-300 keV above ground. The 0.66 second half-life cannot be assigned to any member farther down the decay chain without extraordinary assumptions about the alpha energy versus half-life relationship. Nor can it be assigned to a ^{227}U parent because the same 7.28 and 7.32 MeV peaks were observed to occur with the same 0.66 second half-life in the case of ^{208}Pb bombarded with ^{19}F, in which experiment ^{223}Th was produced by the $(^{19}F, p3n)$ reaction and ^{227}U could not be present.

The 7.28 MeV peak in the spectrum contains a mixture of ^{223}Th and some 25 second ^{221m}Po produced in a direct transfer reaction. On the basis of half-life measurements made at a beam energy of 115 MeV, about one quarter of the combined 7.28 and 7.32 MeV activities belongs to ^{211m}Po. The same estimate was obtained by comparing the combined intensity of these two peaks to that of the 8.68 MeV peak of ^{215}Rn, which indicates that the whole intensity of ^{223}Th, within limits of a few percent, is included in the 7.28 and 7.32 MeV groups. The estimated intensities are 7.28 (60 ± 10%) and 7.32 (40 ± 10%). In bombardments of ^{208}Pb with ^{18}O the ^{223}Th series was produced in good yield (see Fig. 5). Our most accurate value for the half-life of ^{223}Th, $t_{1/2}$ = 0.66 ± 0.01 sec, was obtained from measurements made with this reaction.

2. Radium-219

We assign peaks at 7.980 ± 0.008 MeV and 7.680 ± 0.008 MeV to ^{219}Ra and estimate the relative intensities as 35% and 65%, respectively. In this analysis we allowed for the fact that the 7.98 MeV peak is a mixture of ^{219}Ra and ^{222}Th. The assignment of the 7.68 MeV peak to ^{219}Ra rather than ^{223}Th was made on an intensity argument: namely, that with this choice the total intensity of the ^{219}Ra alpha groups is equal to that of the ^{223}Th and ^{215}Rn peaks, whereas with any other assignment the equilibrium intensity balances would be quite wrong. The assignment of the two peaks to ^{219}Ra was also based on their observation in samples prepared by bombardment ^{208}Pb with ^{16}O; in this case ^{219}Ra could be made by the (^{16}O,αn) reaction and ^{223}Th could not be present.

The ^{208}Pb + ^{16}O reaction was used to make samples for a determination of the ^{219}Ra half-life by observing the decay of the 7.68 and 7.98 MeV peaks

of ^{219}Ra as well as the 8.69 MeV peak of ^{215}Rn. Figure 6 shows alpha spectra from the reaction and Fig. 7 shows some excitation function curves for these peaks. The 7.98 MeV peak is strongly contaminated with ^{222}Th and hence is unsuitable for a half-life measurement. The 7.68 MeV peak was also impure but had a higher percentage of ^{219}Ra. The 8.69 MeV peak of ^{215}Rn is contaminated with 8.698 MeV ^{215}Ra at beam energies above 100 MeV because of the formation of ^{215}Ra from the decay of ^{219}Th produced in a compound nucleus reaction. Half-life measurements of the 7.68 MeV and 8.68 MeV peaks were performed at beam energies which minimized the contributions of these contaminants (87 MeV in the case of the 8.68 MeV peak) and a half-life component of 10 ± 3 milliseconds was determined and assigned to ^{219}Ra. In the study of the $^{208}Pb + ^{14}N$ reaction we observed ^{219}Ra prepared by the $(^{14}N, p2n)$ reaction and measured a half-life of 10 ± 3 msec for the 8.68 MeV peak of ^{215}Rn, in this case with no interference from ^{215}Ra.

3. Radon-215

The 8.68 MeV peak observed in all spectra containing the ^{223}Th decay chain has the expected energy for ^{215}Rn (see Fig. 17). The half-life values of 0.6 sec or 10 msec determined for this peak in the experiments cited above belong to ^{223}Th and ^{219}Ra parent activity respectively. The half-life of ^{215}Rn was determined in the $^{208}Pb + ^{18}O$ experiments by use of the time-to-amplitude converter method discussed at the end of the experimental section: the value was 2.30 ± 0.1 μsec. The off line sorts of the data by use of the MULTIS program also gave accurate values for the intensities of the ^{219}Ra alpha groups which are entered in Table III. Our best measurement of the alpha-particle energy is 8.675 ± 0.008 MeV.

C. The Thorium-222 Decay Chain

There is no published literature on the properties of the ^{226}U decay chain which should follow this sequence:

$$^{226}U \xrightarrow{\alpha} {}^{222}Th \xrightarrow{\alpha} {}^{218}Ra \xrightarrow{\alpha} {}^{214}Rn \xrightarrow{\alpha} {}^{210}Po \xrightarrow[138\ \text{days}]{\alpha} {}^{206}Pb \quad \text{stable}$$

The first two members of this chain might be expected to have half-lives in the range of milliseconds and the radium and radon daughters in the range of microseconds.

In the present study formation of members of this series was expected from four compound nucleus reactions $^{208}Pb(^{22}Ne,4n)^{226}U$, $^{208}Pb(^{16}O,2n)^{222}Th$, $^{208}Pb(^{18}O,4n)^{222}Th$, and $^{208}Pb(^{12}C,2n)^{218}Ra$ and from four "alpha-out" reactions $^{208}Pb(^{22}Ne,\alpha 4n)^{222}Th$, $^{209}Bi(^{19}F,\alpha 2n)^{222}Th$, $^{208}Pb(^{20}Ne,\alpha 2n)^{222}Th$, and $^{208}Pb(^{16}O,\alpha 2n)^{218}Ra$. All these target-projectile combinations were tried (see Table I) and the overall result was that no clear-cut evidence was found for ^{226}U even in the most favorable reaction, which was $^{208}Pb(^{22}Ne,4n)^{226}U$. This can be attributed to the large loss by fission. On the other hand clear proof was obtained for ^{222}Th particularly in the $^{209}Bi + {}^{19}F$ and $^{208}Pb + {}^{20}Ne$ reactions. Spectra from these experiments are shown in Figs. 8 and 10 and the excitation function curves for the main alpha groups are shown in Figs. 9 and 11. The half-lives determined for these groups are shown in Fig. 12.

The alpha groups with energies of 7.98, 8.39, and 9.04 MeV certainly belong to a single series on the basis of their similar excitation functions

and decay curves. This series can only be the $^{222}Th \rightarrow ^{218}Ra \rightarrow ^{214}Ra$ family on the basis of decay energies predicted from trends in decay energy as discussed below and displayed in Fig. 17. Furthermore, the yield maximum at 100 MeV beam energy which is 9 MeV above the estimated Coulomb barrier in the $^{208}Pb + ^{20}Ne$ reaction and 7 MeV below the yield maximum for the ^{221}Th decay chain (discussed later), is reasonable for the production of ^{222}Th by the $^{208}Pb(^{20}Ne,\alpha 2n)$ reaction. We thus make the following assignments: ^{222}Th 7.980 ± 0.010 MeV, ^{218}Ra 8.385 ± 0.008 MeV, ^{214}Rn 9.035 ± 0.010 MeV. The three alpha peaks decay with the same apparent half-life of 3.1 msec because the expected half-lives for ^{218}Ra and ^{214}Rn lie in the microsecond and sub-microsecond region and the ^{222}Th half-life is controlling. The apparent half-life has to be corrected for a distortion caused by the time-of-transport of the recoil activity out of the reaction cell and we estimate the true half-life to be 2.8 ± 0.3 msec. We confirmed the fact that the ^{218}Ra half-life is much shorter by failing to find the 8.385 and 9.035 MeV peaks among the products of the $^{208}Pb + ^{12}C$ reaction.

Small amounts of ^{222}Th were made by the $^{208}Pb(^{22}Ne,\alpha 4n)^{222}Th$ reaction (see Fig. 3) and by the $^{208}Pb(^{16}O,2n)$ reaction (see Figs. 6 and 7). No evidence of production of ^{226}U or ^{222}Th was found by reactions of the "proton-out" type.

The intensity of the ^{222}Th, ^{218}Ra, and ^{214}Rn peaks should be equal, but in our spectra and excitation functions (see Figs. 7, 9, and 11) the relative intensity of the 7.98 MeV group is high. Part of this excess can be attributed to ^{219}Ra contamination of the 7.98 MeV peak but part is an effect of pulse pile up as discussed in Section II. The $^{208}Pb + ^{18}O$ reaction

was used to produce the ^{222}Th series for a coincidence experiment of the type shown in Fig. 2 and discussed in Section II. The ^{222}Th peak at 7.980 MeV was observed in the start spectrum and both the ^{218}Ra peak of 8.385 MeV and the ^{214}Rn peak of 9.035 MeV were observed in equal intensity in the stop spectrum. An off-line sort of the data gave a value of 14 ± 2 μsec for the ^{218}Ra half-life.

The absence of the ^{218}Ra alpha peak in the start spectrum indicated that the ^{214}Rn half-life is too short to be measured by this method. We then made use of a variation of the method, to be described elsewhere (Ref. 10), in which the sum peak of the mother-daughter alpha group was recorded together with the time delay between both pulses. We were able to determine a value of 0.27 ± 0.02 μsec for the ^{214}Rn half-life.

Our results on the ^{222}Th decay chain members are summarized in Table IV. While this work was in progress independent data were obtained by Torgerson and Macfarlane[16] as listed in Table IV.

D. The Thorium-221 Decay Chain

The unknown isotope, ^{225}U, must decay by the following chain of alpha emissions:

$$^{225}U \xrightarrow{\alpha} {}^{221}Th \xrightarrow{\alpha} {}^{217}Ra \xrightarrow{\alpha} {}^{213}Rn \xrightarrow[19\ msec]{\alpha} {}^{209}Po \xrightarrow[103\ y]{\alpha} {}^{205}Pb \quad (3\times10^{7}\ y)$$

The half-lives of ^{225}U and ^{221}Th can be expected to be in the millisecond range while that of ^{217}Ra should be of the order of a few microseconds.

We searched for ^{225}U in experiments done with the most favorable target projectile combinations, which were $^{208}Pb + {}^{22}Ne$, $^{208}Pb + {}^{20}Ne$, and $^{209}Bi + {}^{19}F$, but found no evidence for it; we attribute this to loss of

uranium nuclei by nuclear fission. We found clear evidence for ^{221}Th prepared by the following reactions ^{208}Pb(^{22}Ne,α 5n)^{221}Th, ^{208}Pb(^{20}Ne,α 3n)^{221}Th, ^{209}Bi(^{19}F,α3n)^{221}Th, and ^{208}Pb(^{16}O,3n)^{221}Th. Some information was also obtained from the ^{206}Pb(^{20}Ne,αn)^{221}Th reaction.

The key to the identification of members of the ^{221}Th family is the presence of ^{213}Rn which emits 8.090 MeV alpha particles with a reported 19 msec half-life.[17] In the present work a special attempt was made to remeasure the half-life of ^{213}Rn. A ^{208}Pb target was bombarded with 65 MeV ^{12}C ions to produce ^{217}Ra, which has such a short half-life (1.6 μsec as reported below) that it completely decays before it can be transported from the reaction cell by the helium gas flow. The ^{213}Rn daughter remains in the gas stream and it was possible to collect it on a collector surface cooled by liquid nitrogen. The effects of this collector surface cooling on the spectrum is dramatic as shown in Fig. 13. The ^{212}Rn and ^{213}Rn peaks at 6.269 MeV and 8.090 MeV, respectively are clearly present and a smaller peak has appeared at 7.55 MeV. Half-life measurements of the 8.090 MeV alpha group gave the value $t_{1/2}$ = 25.0 ± 0.2 msec for ^{213}Rn. The 7.55 MeV peak decays with a half-life of 20 ± 5 msec. It may be assigned as a 1% alpha branch from ^{213}Rn.

In the study of the other reactions by the normal technique, the repeated occurrence of alpha groups of energy 7.73 (low intensity), 8.15, 8.47, and 8.99 MeV with excitation functions similar to the 8.09 MeV ^{213}Rn made it possible to assign these peaks to ^{221}Th and ^{217}Ra.

Consider the spectra in Fig. 10 and the yield curves in Fig. 11. The 7.73, 8.09, 8.15, 8.47, and 8.99 MeV peaks all have a maximum yield at 109 MeV,

18 MeV above the estimated Coulomb barrier, which is quite reasonable for a (^{20}Ne,α3n) reaction. The ^{209}Bi + ^{19}F reactions provide similar evidence for these alpha groups and for their association as a family. See Figs. 8 and 9. It was impossible to assign any of these peaks to ^{225}U and it was concluded that ^{221}Th is the primary product and parent of the observed series. This was confirmed by a bombardment of a ^{208}Pb target with ^{16}O in which ^{225}U could not be formed and ^{221}Th could easily be made by the ^{208}Pb(^{16}O,3n) ^{221}Th reaction. The same alpha peaks were present as shown by the spectra in Fig. 6 and the yield curves in Fig. 7. The yield maximum at 87 MeV beam energy, 12 MeV above the Coulomb barrier, agrees with a compound nucleus reaction rather than an "alpha-out" reaction.

We assign the 8.47 MeV alpha group to ^{221}Th as it is the most reasonable for the ^{221}Th ground state transition. See Fig. 17. We also assign the 8.47 MeV and 7.73 MeV groups to ^{221}Th. Our best values for the ^{221}Th alpha-group energies and intensities are: 8.145 ± 0.010 MeV 56 ± 3%, 8.470 ± 0.008 MeV 39 ± 2%, and 7.725 ± 0.010 MeV 6 ± 1%. These intensity values were determined by an off-line sort of data obtained by an experiment of the type diagramed in Fig. 2 and described in Section II. The ^{221}Th alpha groups in the start spectrum associated with 8.995 MeV alpha particles from ^{217}Ra in the stop spectrum are shown in Fig. 14. A different sort of the same data gave the ^{217}Ra half-life value of 1.6 ± 0.2 μsec as shown in Fig. 15. Torgerson and Macfarlane[16] made a prior measurement of the ^{217}Ra half-life by a similar technique.

The value for the ^{221}Th half-life came from a measurement of the decay of the 8.47 MeV group of ^{221}Th and of the 8.99 MeV group of ^{218}Ra

and the 8.15 MeV group of ^{214}Rn (in equilibrium) in samples prepared by the ^{208}Pb(^{16}O,3n)^{221}Th reaction. The results are shown in Fig. 16. The experimental value of 2.1 msec is an upper limit influenced by the finite time of transport of the recoil activity from the reaction cell. When a correction is made for this effect, the shorter value of 1.8 ± 0.3 msec is obtained.

In accordance with the measured short half-life of ^{217}Ra we did not observe the 8.99 MeV peak in the spectra taken in the ^{208}Pb + ^{12}C reaction in which ^{219}Ra should be made in large cross section by the ^{208}Pb(^{12}C,3n)^{217}Ra reaction. (See Fig. 13).

While this work was in progress we learned of the independent work of Torgerson and Macfarlane[16,18] who obtained similar results for ^{221}Th and ^{217}Ra as shown by the entries in Table IV.

E. Comments on the Uranium-224 Decay Chain

It is certain that ^{224}U is an alpha emitter decaying through the sequence:

$$^{224}\text{U} \xrightarrow{\alpha} {}^{220}\text{Th} \xrightarrow{\alpha} {}^{216}\text{Ra} \xrightarrow{\alpha} {}^{212}\text{Rn} \xrightarrow[25\ \text{min}]{\alpha} {}^{208}\text{Po} \xrightarrow[2.9\ \text{y}]{\alpha} {}^{204}\text{Pb}\ (\text{stable})$$

The uranium isotope is expected to have a half-life of a fraction of a millisecond and the thorium and radium daughters should be even shorter lived. Because of these short half-lives and because of large losses from fission competition we would expect at best to see traces of the ^{224}U family produced by ^{208}Pb(^{20}Ne,4n)^{224}U and ^{209}Bi(^{19}F,4n)^{224}U reaction.

In Figs. 8 and 10 there are trace peaks at 8.83 and 9.38 MeV which may be radiations of ^{220}Th and ^{216}Ra, respectively, kept alive by ^{224}U which

is decaying with a half-life of a few tenths of a millisecond. The expected 8.3 MeV alpha particles of ^{224}U are invisible because of the presence of other peaks of similar energy.

These are very tentative assignments requiring further experimental proof but the following arguments can be made to support them: (1) the excitation function maxima in Figs. 9 and 11 are at the proper energy, (2) the alpha particle energies fit correctly on the curves for radium and thorium in Fig. 17. We particularly emphasize that a 9.38 MeV energy is unusually high so that the possible assignments are extremely limited, as can be seen in the alpha systematics figure. In fact the only other possibility is ^{215}Fr which[10] has its main alpha groups at 9.36 MeV. However, ^{215}Fr could appear in our spectra only as the granddaughter of ^{223}Pa prepared by a "proton-out" reaction and should have a yield maximum at a beam energy 25 to 30 MeV higher than observed for the 9.38 MeV group. Furthermore, we observed that 9.38 MeV alpha pulses occurred only during the beam burst and the first millisecond afterward, indicating a controlling half-life of less than 1 msec which is much less than the 6 msec half-life of ^{223}Pa.

F. Other Peaks in Spectra

In some of the figures there occur labeled peaks indicating the presence of odd-Z nuclides even though the compound nucleus is even Z. These peaks are prominent only in the $^{209}Bi + ^{19}F$ case where there are strong francium and astatine isotope peaks which probably are the result of partial transfer reactions, reflecting the substructures in the ^{19}F projectile. We do not discuss this interpretation in the present paper. The ^{217}Fr and ^{213}At peaks which

appear in several of the spectra are probably the result of "proton-out" reactions producing ^{221}Ac which decays through the chain:

$$^{221}Ac \xrightarrow[52\ \text{msec}]{\alpha} {}^{217}Fr \xrightarrow[22\ \mu\text{sec}]{\alpha} {}^{213}At \xrightarrow[0.11\ \mu\text{sec}]{\alpha} {}^{209}Bi$$

This chain is discussed in another paper.[10]

In addition there are few minor peaks for which we have made no definite identification. The principal ones of these are the 8.86, 7.56, and 7.74 MeV trace peaks appearing in Fig. 3 ($^{208}Pb + {}^{22}Ne$).

IV. DISCUSSION OF ALPHA-DECAY REGULARITIES

It is well established that alpha-particle energies for ground state transitions in the decay of even-Z isotopes vary in a regular fashion when values for isotopes of individual elements are plotted against neutron number. These regularities have not been well mapped out for neutron numbers just above the 126 neutron shell but the recently-obtained data on the isotopes of thorium, radium, and radon make it possible to draw in the regularities with considerably more confidence. We have done this in Fig. 17 and have extrapolated the trends in experimental data to give our best estimate for those isotopes still not measured.

It is of some interest to compare these decay values with the predictions of various mass formulae or semiempirical methods of estimation of nuclear masses and decay energy. In Table V we compare our estimated Q values, converted from the squares in Fig. 17 with those predicted by Myers and Swiatecki,[19] Garvey et al.,[20] and Viola and Seaborg.[21] In Table VI we show the comparison of our experimental alpha Q values with these same authors.

It is also of interest to compare our half-life values for even-even nuclei with predictions based on the semiempirical relationship

$$t_{1/2} = A_Z Q_{eff}^{-1/2} + B_Z \qquad (1)$$

where $t_{1/2}$ is the partial half-life in seconds, Q_{eff} is the alpha energy in MeV corrected for recoil energy and for screening of the atomic elections, and A_Z and B_Z are empirical constants. It has been shown[22,23] that this simple expression is capable of correlating the half-lives of even nuclei over a range of 16 orders of magnitude or more. Our new half-lives fall in the microsecond range and represent a test of the extrapolation of this correlation into a region of very short decay periods.

We make this comparison for three isotopes and list predicted half-lives for three additional isotopes in Table VII. The predicted values are based on the most recent set of empirical constants taken from the work of Viola and Seaborg.[21]

V. ACKNOWLEDGMENTS

One of us (KV) expresses his appreciation to the Committee of Natural Sciences of Finland for financial support during part of the work recorded here. One of us (JB) expresses his thanks for a fellowship from the North Atlantic Treaty Organization. We are indebted to the crew of the HILAC for their indispensable assistance and to A. A. Wydler and R. G. Leres for help on electronic problems. We acknowledge also our debt of Dr. Lloyd Robinson for his contribution to the PDP-7 computer system and for writing the special MULTID and MULTIS programs mentioned in the text.

REFERENCES

1. W. Treytl and K. Valli, Nucl. Phys. A97, 405 (1967).
2. K. Valli, M. J. Nurmia, and E. K. Hyde, Phys. Rev. 159, 1013 (1967).
3. K. Valli, E. K. Hyde, and W. Treytl, J. Inorg. Nucl. Chem. 29, 2503 (1967).
4. K. Valli, W. Treytl, and E. K. Hyde, Phys. Rev. 161, 1284 (1967).
5. K. Valli, W. J. Treytl, and E. K. Hyde, Phys. Rev. 167, 1094 (1968).
6. K. Valli and E. K. Hyde, Phys. Rev. 176, 1377 (1968); additional information on the helium jet technique is given by R. D. Macfarlane et al., Nucl. Instru. and Meth. 73, 285 (1969).
7. W. W. Meinke, A. Ghiorso, and G. T. Seaborg, Phys. Rev. 75, 314 (1949); 81, 782 (1951); and 85, 429 (1952).
8. C. P. Ruiz, University of California Lawrence Radiation Laboratory report UCRL-9511, 1961, (unpublished), abstracted in C. M. Lederer, J. M. Hollander, and I. Perlman Table of Isotopes, 6th edition, (John Wiley and Sons, Inc.), New York, 1967.
9. R. L. Hahn, M. F. Roche, and K. S. Toth, Phys. Rev. 182, 1329 (1969).
10. K. Valli, E. K. Hyde, and J. Borggreen, paper in preparation (1969).
11. L. C. Northcliffe, Phys. Rev. 120, 1744 (1960).
12. L. C. Northcliffe, Ann. Rev. Nucl. Sci. 13, 67 (1963).
13. A. Rytz, Phys. Acta. 34, 240 (1961).
14. D. A. Orth, University of California Radiation Laboratory report UCRL-1059, 1951.
15. P. A. Tove, Arkiv Fysik 13, 549 (1958).
16. D. F. Torgerson and R. D. Macfarlane, private communication, 1969; D. F. Torgerson Ph.D. Thesis, McMaster University, Canada (1969).

17. R. D. Griffioen and R. D. Macfarlane, Bull. Am. Phys. Soc. 7, 541 (1962).

18. D. F. Torgerson and R. D. Macfarlane, Bull. Am. Phys. Soc. 13, 1370 (1968).

19. W. D. Myers and W. J. Swiatecki, Nucl. Phys. 81, 1 (1966); University of California Lawrence Radiation Laboratory Report UCRL-11980.

20. G. T. Garvey, W. J. Gerace, R. L. Jaffe, I. Talmi, and I. Kelson, Rev. Mod. Phys. 41, No. 4, Pt. II, pp S1-S80, Oct. (1969).

21. V. E. Viola and G. T. Seaborg, J. Inorg. Nucl. Chem. 28, 697 (1966) and 28, 741 (1966).

22. C. J. Gallagher and J. O. Rasmussen, J. Inorg. Nucl. Chem. 3, 333 (1967).

23. A. Bohr, P. O. Fröman, and B. R. Mottelson, Dan. Mat. fys. Medd. 29, No. 10 (1955).

Table I. General summary of target-projectile combinations

Target, projectile and compound nucleus	Level of usefulness for identification of thorium decay chains		
	High	Moderate	Low
$^{208}Pb + {}^{22}Ne \longrightarrow {}^{230}U$	^{224}Th, ^{223}Th	^{222}Th, ^{221}Th	
$^{208}Pb + {}^{20}Ne \longrightarrow {}^{228}U$	^{222}Th, ^{221}Th	^{223}Th	^{220}Th
$^{209}Bi + {}^{19}F \longrightarrow {}^{228}U$		^{222}Th, ^{221}Th	
$^{208}Pb + {}^{16}O \longrightarrow {}^{224}Th$	^{221}Th		^{222}Th, ^{219}Ra
$^{208}Pb + {}^{18}O \longrightarrow {}^{226}Th$	^{223}Th, ^{222}Th		
$^{209}Bi + {}^{22}Ne \longrightarrow {}^{231}Np$		^{223}Th	
$^{206}Pb + {}^{20}Ne \longrightarrow {}^{226}U$			^{221}Th
$^{208}Pb + {}^{19}F \longrightarrow {}^{227}Pa$			^{223}Th, ^{224}Th
$^{205}Tl + {}^{22}Ne \longrightarrow {}^{227}Pa$			^{223}Th, ^{224}Th
$^{209}Bi + {}^{16}O \longrightarrow {}^{225}Pa$			^{221}Th
$^{208}Pb + {}^{14}N \longrightarrow {}^{222}Ac$			^{219}Ra
$^{209}Bi + {}^{12}C \longrightarrow {}^{221}Ac$			^{219}Ra

Table II. Alpha groups of the ^{228}U decay chain

Nuclide	Meinke et al. Alpha energy (MeV)	Orth Alpha energy (MeV)	Ruiz Alpha energy (MeV)	%	This work Alpha energy (MeV)	%
^{223}U	6.72	6.67 ± 0.02	6.68 ± 0.01	70 ± 4		
			6.59 ± 0.01	29 ± 4		
			6.44[a]	0.7 ± 0.3[b]		
			6.40[a]	0.5 ± 0.2[b]		
^{224}Th	7.20	7.13 ± 0.02	7.17 ± 0.01	80 ± 2	7.17 ± 0.01	81 ± 3
			6.99 ± 0.01	19 ± 2	7.00 ± 0.01	19 ± 3
			6.77	1.5 ± 0.6[b]		
			6.70	0.5 ± 0.3[b]		
^{220}Ra	7.49	7.43 ± 0.03	7.45	99	7.455 ± 0.01	
			6.90[a]	1 ± 0.4		
^{216}Rn	8.07	8.01 ± 0.03	8.04 ± 0.01		8.05 ± 0.01	

[a] Existence of group deduced from γ-ray data

[b] Abundance deduced from γ-ray data

UCRL-18992

Table III. Alpha-decay for ^{227}U decay chain

Nuclide	Meinke et al.[a]		Tove[c]	Hahn et al.[b]			This work		
	Eα (MeV)	$T_{\frac{1}{2}}$ (min)	$T_{\frac{1}{2}}$ (sec)	Eα (MeV)	%	$T_{\frac{1}{2}}$ (min)	Eα (MeV)	%	$T_{\frac{1}{2}}$
^{227}U	6.8 ± 0.1	1.3 ± 0.3		6.87 ± 0.02		1.1 ± 0.1			
^{223}Th	7.55 ± 0.1		0.9 ± 0.1	7.33 ± 0.02			7.285 ± 0.010	60 ± 10	0.66 ± 0.01 sec
							7.315 ± 0.010	40 ± 10	0.66 ± 0.01 sec
^{219}Ra	8.0 ± 0.1			7.99 ± 0.02	30 ± 10		7.980 ± 0.010	35 ± 2	10 ± 3 msec
				7.70 ± 0.02	70 ± 10		7.675 ± 0.010	65 ± 5	10 ± 3 msec
^{215}Rn	8.6 ± 0.1			8.67 ± 0.02			8.675 ± 0.008	100	2.30 ± 0.1 μsec
^{211}Po	7.434			7.46 ± 0.02			7.448 ± 0.010		

[a] see reference 4
[b] see reference 9
[c] see reference 15

UCRL-18992

Table IV. Summary of data on ^{222}Th, and ^{221}Th decay families

Nuclide	This work			Torgerson and Macfarlane[a]		
	α energy (MeV)	Abundance (%)	Half-life	α energy (MeV)	Abundance (%)	Half-life
			thorium-222 family			
^{222}Th	7.980 ± 0.010	100	2.8 ± 0.3 msec	7.984 ± .008	100	4 ± 1 msec
^{218}Ra	8.385 ± 0.010	100	14 ± 2 μsec	8.392 ± .008	100	
^{214}Rn	9.035 ± 0.010	100	0.27 ± 0.02 μsec	9.040 ± 0.020	100	
			thorium-221 family			
^{221}Th	8.470 ± 0.010	30 ± 5	1.8 ± 0.3 msec	8.472 ± 005		1.68 ± 0.08 msec
	8.145 ± 0.010	62 ± 5		8.146 ± 005		
	7.73 ± 0.01	8 ± 3		7.733 ± 008		
^{217}Ra	8.995 ± 0.010		1.6 ± 0.2 μsec	8.990 ± 008		4 ± 1 μsec
^{213}Rn	8.085 ± 0.010	99	25.0 ± 0.2 msec			
	7.55 ± 0.015	1				

[a] reference 16, 18

Table V. Comparison of estimated Q values

	This work		Garvey[a]	Myers[b] Swiatecki	Viola[c] Seaborg
Isotope	Alpha energy (MeV)	Q-value (MeV)	Q-value (MeV)	Q-value (MeV)	Q-value (MeV)
^{216}U	8.38 ± 0.05	8.54	9.40	7.71	
^{217}U	8.21 ± 0.05	8.36	8.81	7.51	
^{218}U	8.63 ± 0.05	8.79	8.74	7.32	
^{219}U	9.70 ± 0.05	9.89	10.17	8.82	
^{220}U	10.00 ± 0.08	10.18	10.98	10.32	
^{221}U	9.65 ± 0.08	9.83	10.38	10.08	
^{222}U	9.15 ± 0.08	9.33	9.62	9.85	
^{223}U	8.80 ± 0.05	8.98	8.98	9.38	9.07
^{224}U	8.32 ± 0.05	8.47	8.59	8.68	8.66
^{225}U	7.98 ± 0.05	8.12	8.10	7.93	8.06
^{226}U	7.50 ± 0.05	7.68	7.62	7.31	7.64
^{227}U	7.17	7.30	7.16	6.96	7.08
^{218}Th	9.70 ± 0.08	9.88	10.55	9.60	9.96
^{219}Th	9.33 ± 0.05	9.50	10.06	9.35	9.58
^{220}Th	8.82 ± 0.05	8.98	9.26	9.12	8.98
^{223}Th	7.65 ± 0.05	7.79	7.66	7.87	

[a] Reference 20
[b] Reference 19
[c] Reference 21

Table VI. Alpha Q-values

	Experimental this work (MeV)	Predictions Garvey[a] (MeV)	Myers Swiatecki[b]	Viola[c] (MeV)
^{221}Th	8.62	8.66	8.87	8.71
^{222}Th	8.13	8.19	8.51	8.23
^{215}Ra	8.86	8.94	7.34	
^{216}Ra	9.56	9.79	8.85	
^{217}Ra	9.17	9.26	8.59	
^{218}Ra	8.54	8.47	8.35	
^{219}Ra	8.13	7.98	8.10	
^{220}Ra	7.60	7.47	7.86	

[a] reference 20

[b] reference 29

[c] reference 21

Table VII. Half-lives of even-even isotopes

Isotope	Half-life	
	Experimental this work	Predicted by equation (1)
^{222}Th	2.8 msec	1.8 msec
^{220}Th	--------	5.6 μsec[a]
^{218}Th	--------	38 nsec[a]
^{218}Ra	14 μsec	34 μsec
^{216}Ra	--------	87 nsec[b]
^{214}Rn	250 nsec	96 nsec

[a]based on estimated α-decay energy taken from column 3 of Table V.

[b]based on estimated α-particle energy of 9.38 MeV (Fig. 17).

FIGURE CAPTIONS

Fig. 1 Section of the chart of the nuclides indicating the group of nuclides just above the 126-neutron shell with which this paper is concerned. Families of alpha emitters on which new information is presented are outlined in black borders. The stable nuclides are outlined in broken lines. These were used as targets.

Fig. 2 Schematic diagram of electronics used to study time correlation of alpha particles from a single detector. TAC stands for time-to-amplitude converter. The time sequence of pulseforms at points A, B, C, etc. in the diagram is displayed in the lower part of the figure.

A. Two linear (energy) signals.

B. The analogous time signals.

C. Gate signal generated if the start pulse is accepted by the TAC, i.e. if the TAC is not busy.

D. Gate signal, generated if the stop pulse is accepted by the TAC, i.e. if it has been proceeded by a (accepted) start pulse within the time range of the TAC.

E. The linear signal corresponding to the "start α" after passing first gate.

F. The same (start α) stretched for a time equal to the TAC time range.

G. Section of this stretched signal gated through to the analyzer by the valid stop signal D.

H. Linear signal corresponding to the "stop α" gated through to the analyzer by the valid stop signal (D).

J. The TAC output proportional to the time elapsed between the emission of the two α-particles (B).

Fig. 3 Spectra of alpha particles emitted by products isolated from ^{208}Pb targets bombarded with 97 MeV ^{22}Ne ions (upper curve) and with 115 MeV ^{22}Ne ions (lower curve).

Fig. 4 Yield of individual members of ^{224}Th and ^{223}Th decay chains as a function of ^{22}Ne beam energy for the reaction system $^{208}Pb + ^{22}Ne$.

Fig. 5 Spectra of alpha particles emitted by products isolated from ^{208}Pb targets bombarded with 130 MeV ^{18}O ions (upper curve) and with 108 MeV ions (lower curve).

Fig. 6 Spectra of alpha particles emitted by products isolated from ^{208}Pb targets bombarded with 87 MeV ^{16}O ions (upper curve) and 92 MeV ^{16}O ions (lower curve).

Fig. 7 Yield of individual products as a function of ^{16}O beam energy for the reaction system $^{208}Pb + ^{16}O$.

Fig. 8 Spectra of alpha aprticles emitted by products isolated from ^{209}Bi targets bombarded with 127 MeV ^{19}F ions (upper curve) and 100 MeV ^{19}F ions (lower curve).

Fig. 9 Yield of individual members of ^{222}Th and ^{221}Th decay families and of a few other products as a function of ^{19}F beam energy for the reaction system $^{209}Bi + ^{19}F$. For curves indicated by (R) use right scales.

Fig. 10 Spectra of alpha particles emitted by products isolated from ^{208}Pb targets bombarded with 106 MeV ^{20}Ne ions (upper curve) and 123 MeV ^{20}Ne ions (lower curve).

Fig. 11 Yield of individual members of the ^{222}Th and ^{221}Th families and of a few other products as a function of ^{20}Ne beam energy for the reaction system, $^{208}Pb + ^{20}Ne$. For curves indicated by (R) use right scales.

Fig. 12 Decay curves of ^{222}Th family members produced in the ^{208}Pb + ^{20}Ne reaction. The "growth" part of the curve is caused by the time-of-transport of the products from reaction cell to the counting chamber. The 8.68 MeV peak is ^{215}Rn. The end of the beam pulse occurred at 6 msec in this time scale.

Fig. 13 Spectra of alpha particles emitted by products isolated from ^{208}Pb bombarded with 66 MeV ^{12}C ions. The products were collected on a surface cooled to liquid nitrogen temperature (upper curve) and at room temperature (lower curve). The broadness of the peak for the 25 min ^{212}Rn is caused by the deposition of a layer of pump oil on the sample.

Fig. 14 Alpha groups of ^{221}Th in start spectrum of TAC experiment (see Fig. 2) done on products of ^{208}Pb + ^{16}O reaction. This spectrum is the result of a data sort with the condition imposed that the stop alpha particle have an energy of 8.995 MeV (^{217}Ra).

Fig. 15 Time relationship between ^{221}Th alpha particles of 8.470 MeV and 8.145 MeV and ^{217}Ra alphas of 8.995 MeV.

Fig. 16 Decay curves for ^{221}Th and ^{217}Ra alpha peaks studied in the reaction of ^{208}Pb with 87 MeV ^{16}O. When a correction is applied for the time-of-transport of the products in the helium gas stream the apparent half-life of ^{221}Th shortens to 1.8 ± 0.3 msec. The zero of the time scale is the end of the beam pulse.

Fig. 17 Systematic trends in alpha particle energies for ground state transitions as a function of neutron number. Even and odd elements are

included on left side of figure but only even-Z elements are shown to the right of the peak. Experimental data are shown by solid dots, estimated data by open squares and broken lines.

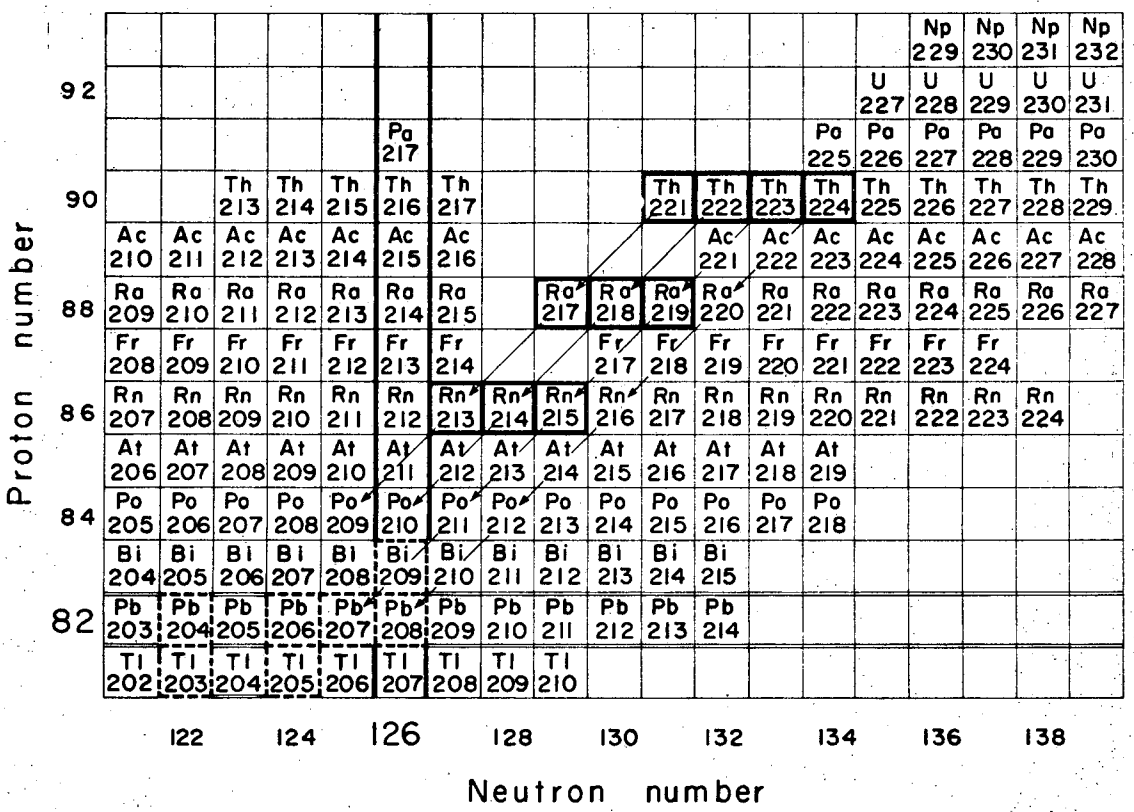
Proton number
92
90
88
86
84
82
122
124
126
128
130
132
134
136
138
Neutron number
XBL6910-3949

Fig. 1

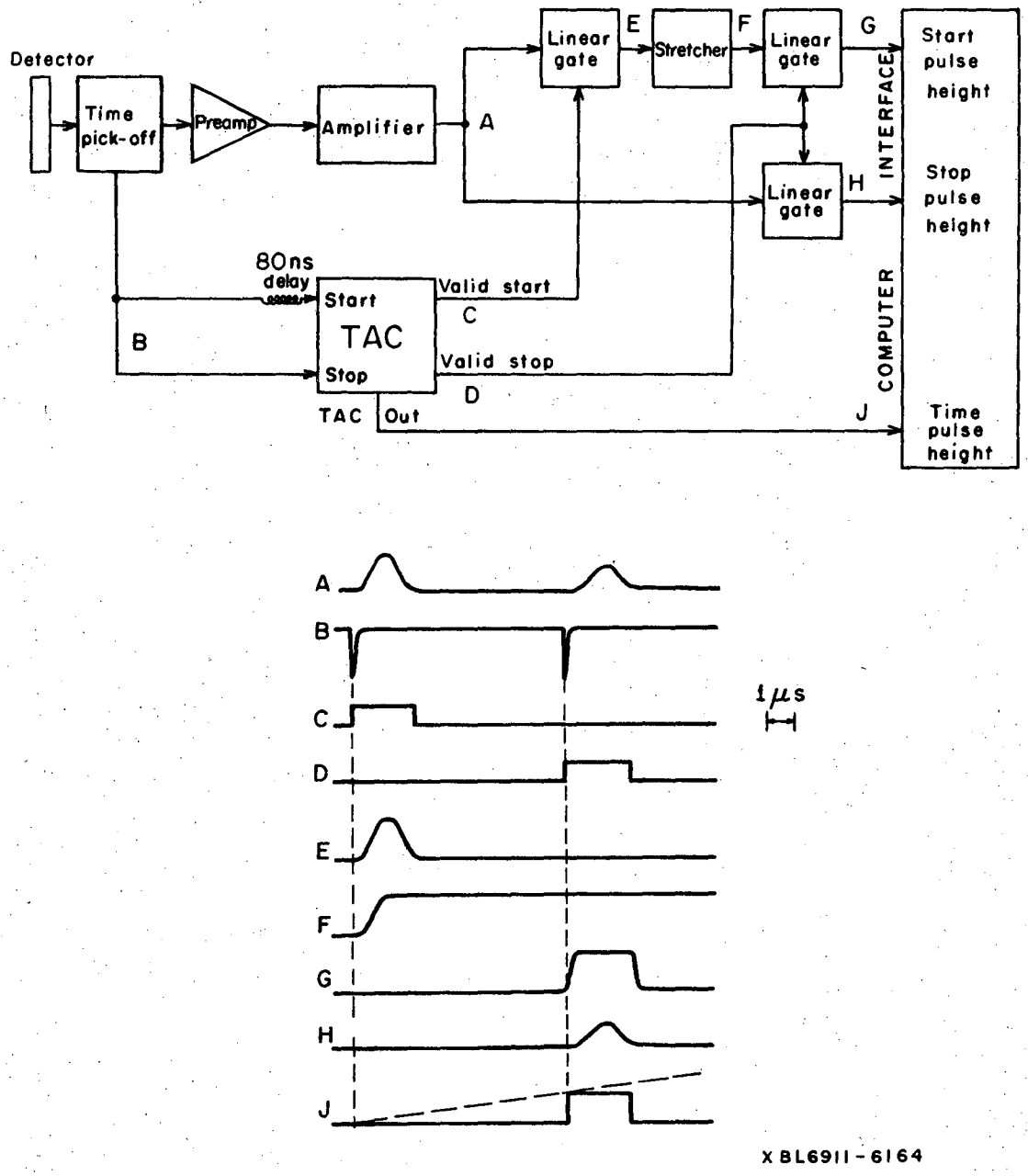
Detector
Time pick-off
Preamp
Amplifier
A
Linear gate
E
Stretcher
F
Linear gate
G
Start pulse height
INTERFACE
Linear gate
H
Stop pulse height
80ns delay
Start
TAC
Stop
Valid start
C
Valid stop
D
B
TAC Out
J
COMPUTER
Time pulse height
A
B
C
D
E
F
G
H
J
1 μs
XBL6911-6164

Fig. 2

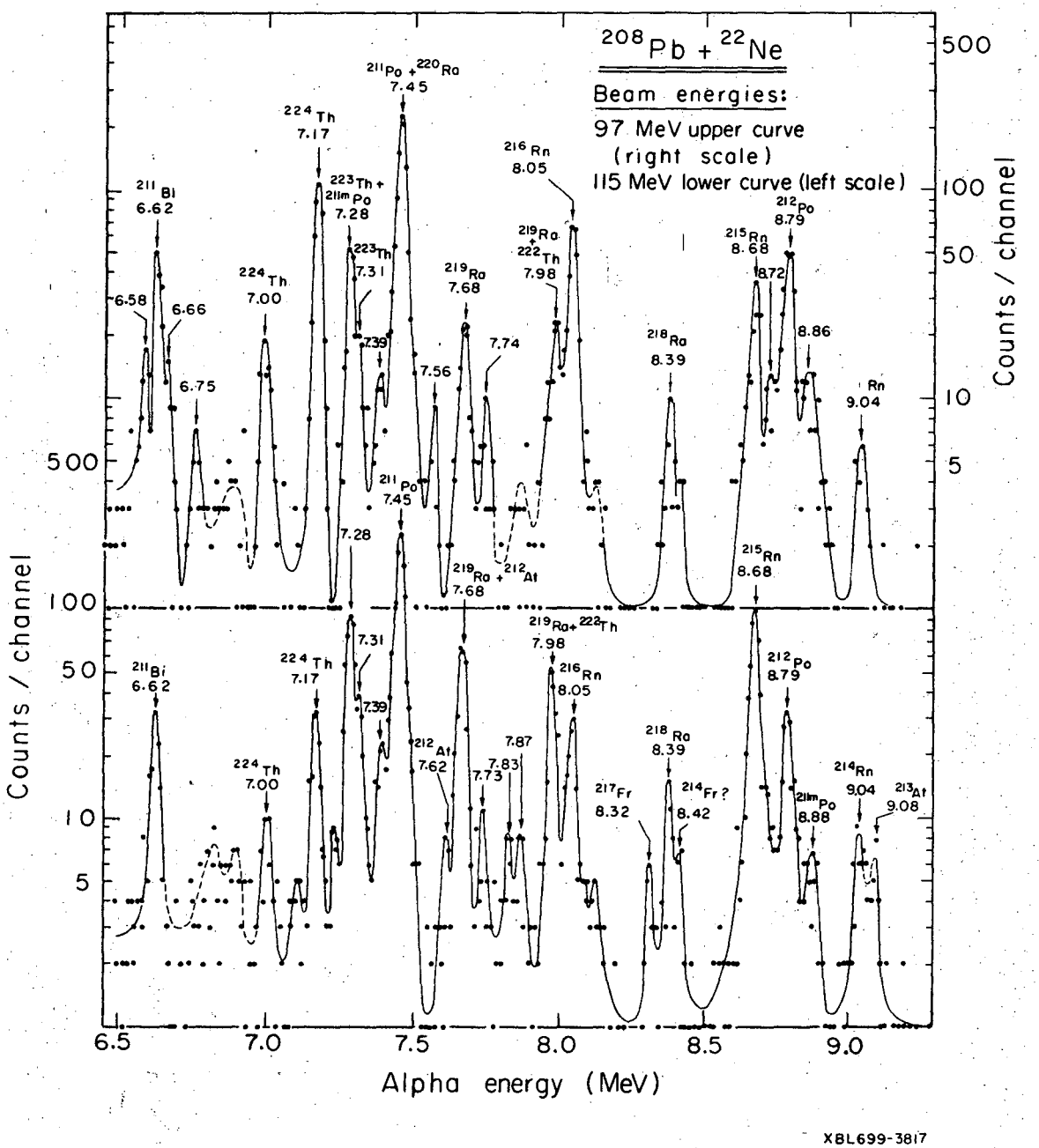
208Pb + 22Ne
Beam energies:
97 MeV upper curve
(right scale)
115 MeV lower curve (left scale)
Counts / channel
Alpha energy (MeV)
211Bi 6.62
6.58
6.66
6.75
224Th 7.00
224Th 7.17
223Th + 211mPo 7.28
223Th 7.31
7.39
211Po + 220Ra 7.45
7.56
219Ra 7.68
7.74
216Rn 8.05
219Ra + 222Th 7.98
218Ra 8.39
215Rn 8.68
8.72
212Po 8.79
8.86
Rn 9.04
212At 7.62
7.73
7.83
7.87
217Fr 8.32
214Fr ? 8.42
211mPo 8.88
214Rn 9.04
213At 9.08
XBL699-3817

Fig. 3

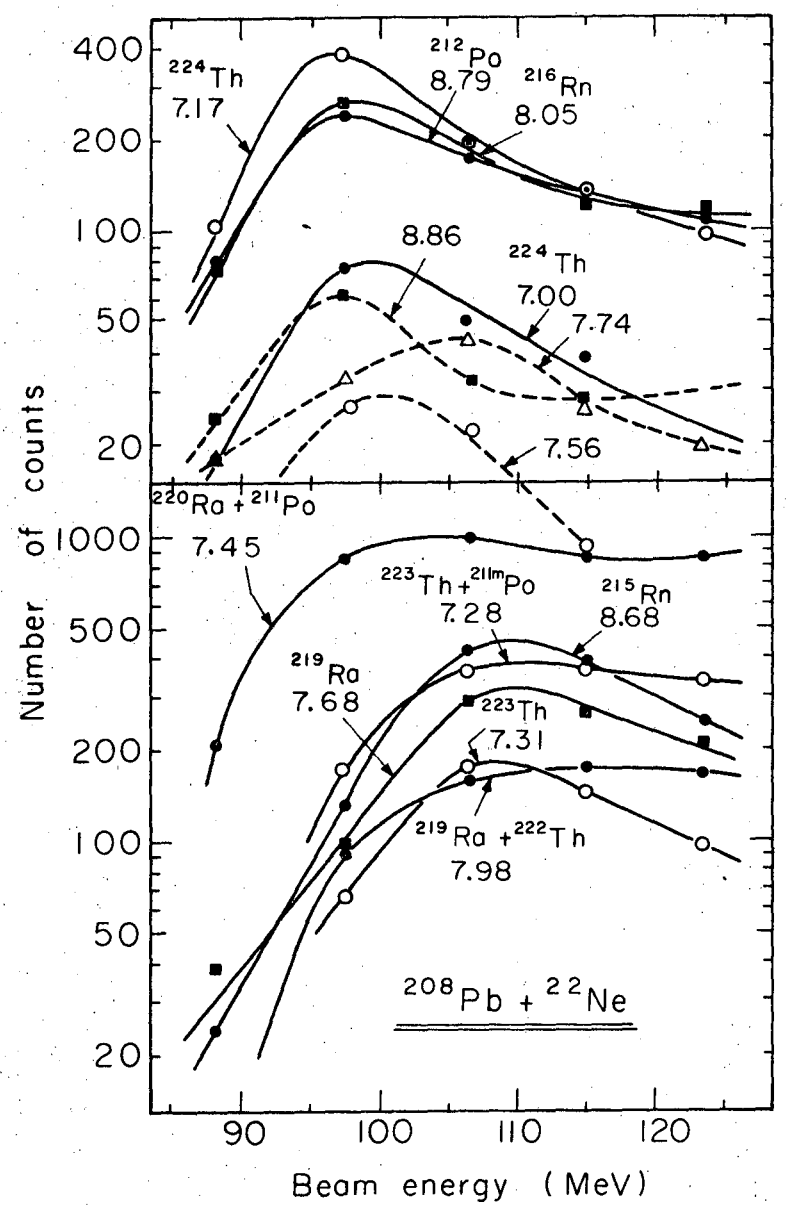

XBL699-3816

Fig. 4

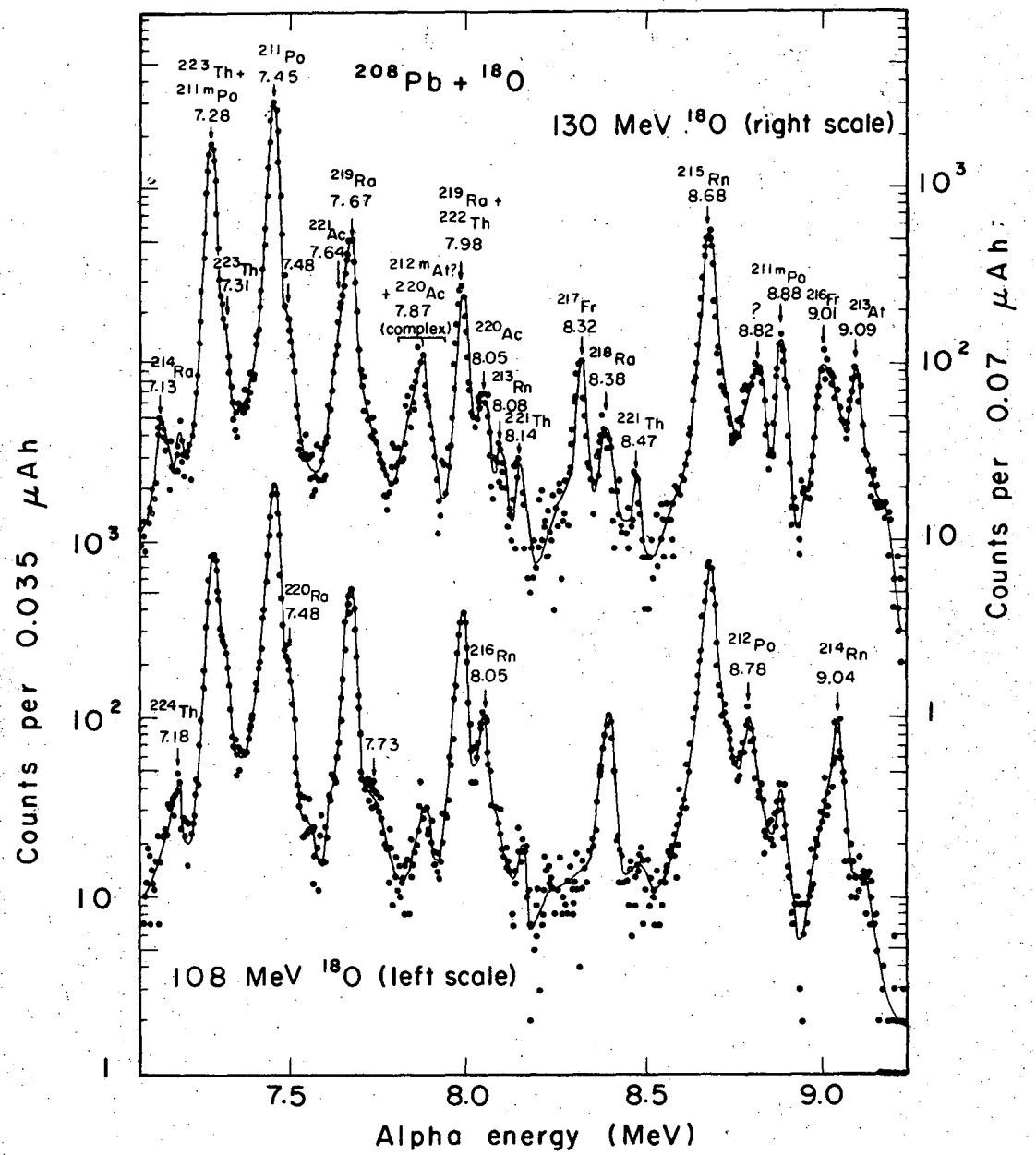
208Pb + 18O
130 MeV 18O (right scale)
108 MeV 18O (left scale)
223Th + 211mPo 7.28
211Po 7.45
219Ra 7.67
221Ac 7.64
7.48
223Th 7.31
212mAt? + 220Ac 7.87 (complex)
219Ra + 222Th 7.98
220Ac 8.05
213Rn 8.08
221Th 8.14
217Fr 8.32
218Ra 8.38
221Th 8.47
215Rn 8.68
211mPo 8.88
? 8.82
216Fr 9.01
213At 9.09
214Ra 7.13
224Th 7.18
220Ra 7.48
7.73
216Rn 8.05
212Po 8.78
214Rn 9.04
Counts per 0.035 μAh
Counts per 0.07 μAh
Alpha energy (MeV)
XBL6911-6165

Fig. 5

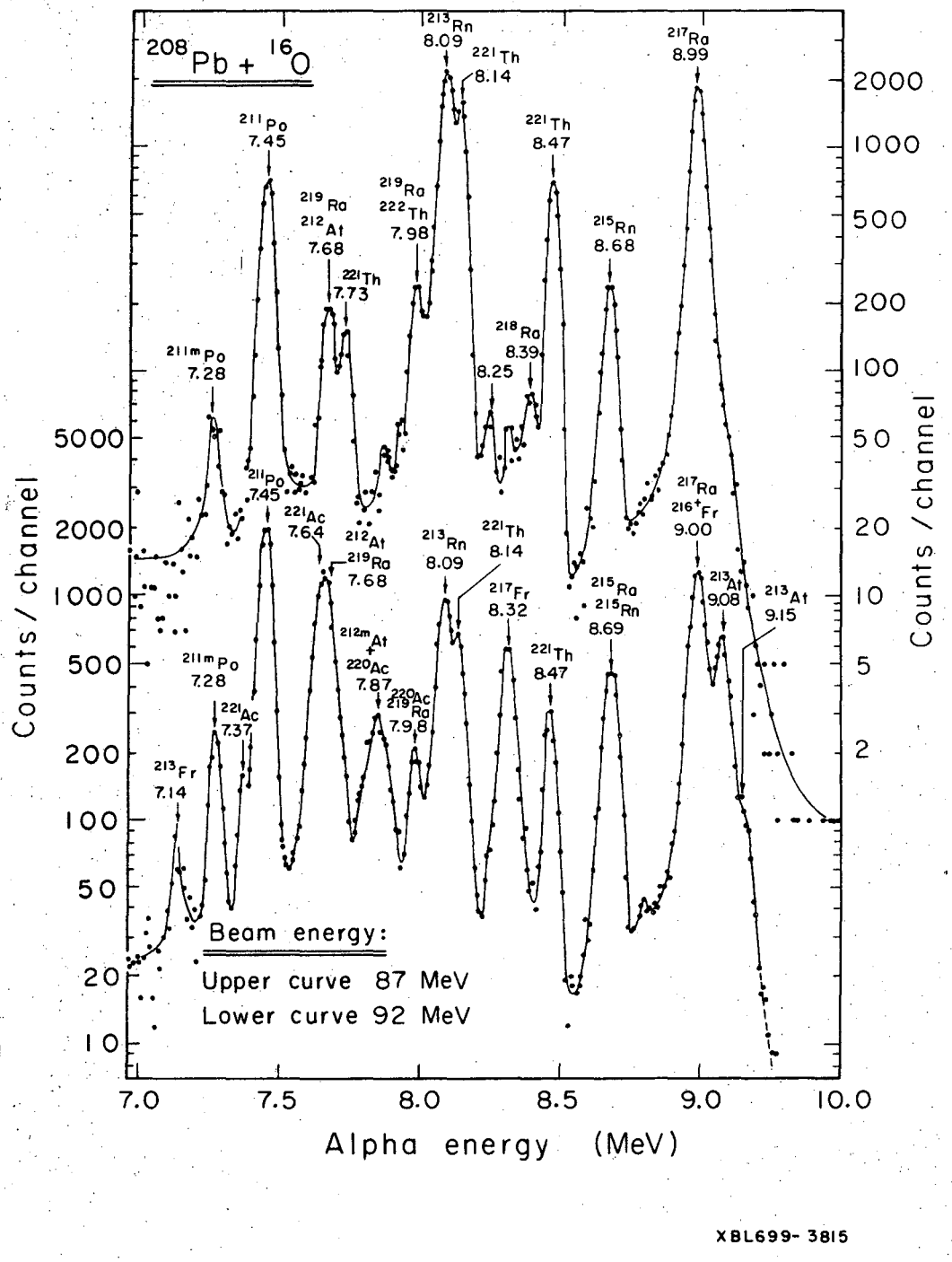

XBL699-3815

Fig. 6

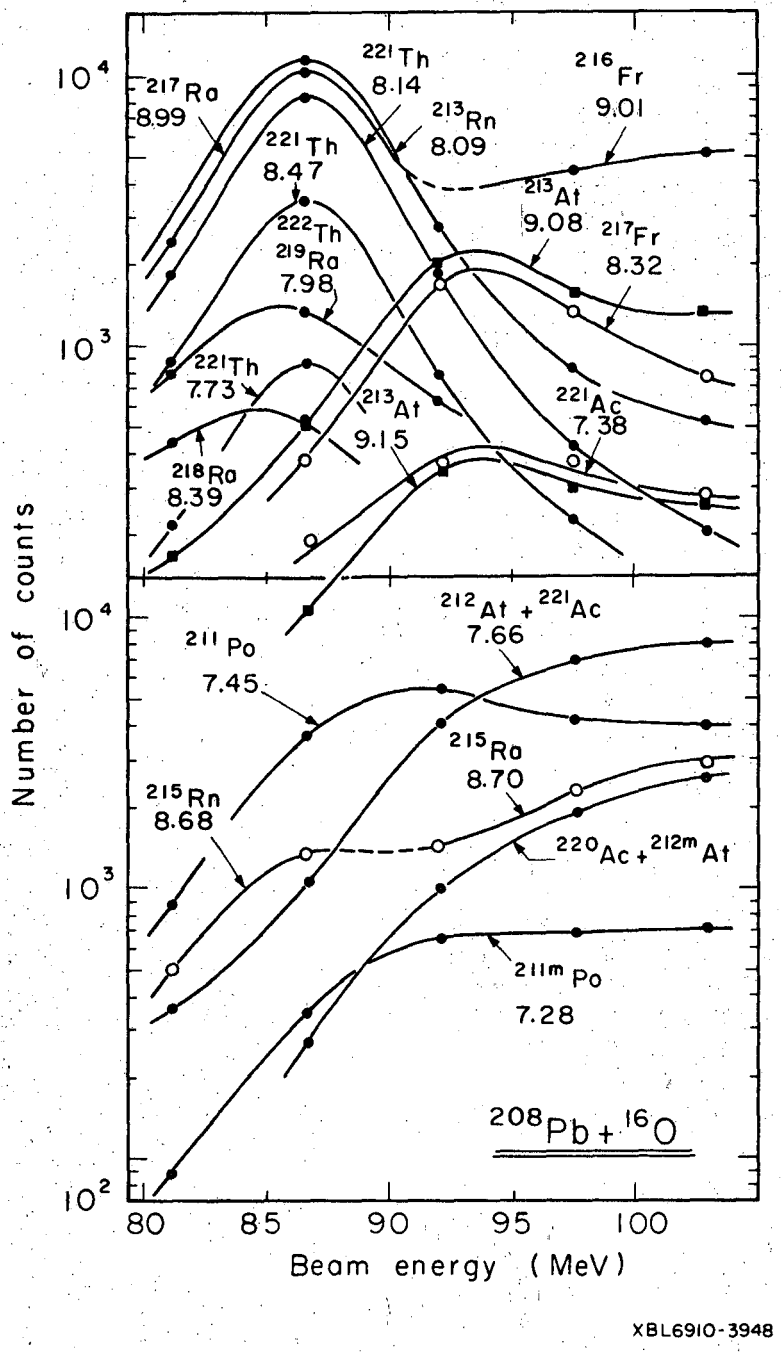
Number of counts
Beam energy (MeV)
^{217}Ra 8.99
^{221}Th 8.14
^{213}Rn 8.09
^{216}Fr 9.01
^{221}Th 8.47
^{213}At 9.08
^{217}Fr 8.32
^{222}Th
^{219}Ra 7.98
^{221}Th 7.73
^{213}At 9.15
^{221}Ac 7.38
^{218}Ra 8.39
^{212}At + ^{221}Ac 7.66
^{211}Po 7.45
^{215}Ra 8.70
^{215}Rn 8.68
^{220}Ac + ^{212m}At
^{211m}Po 7.28
^{208}Pb + ^{16}O
XBL6910-3948

Fig. 7

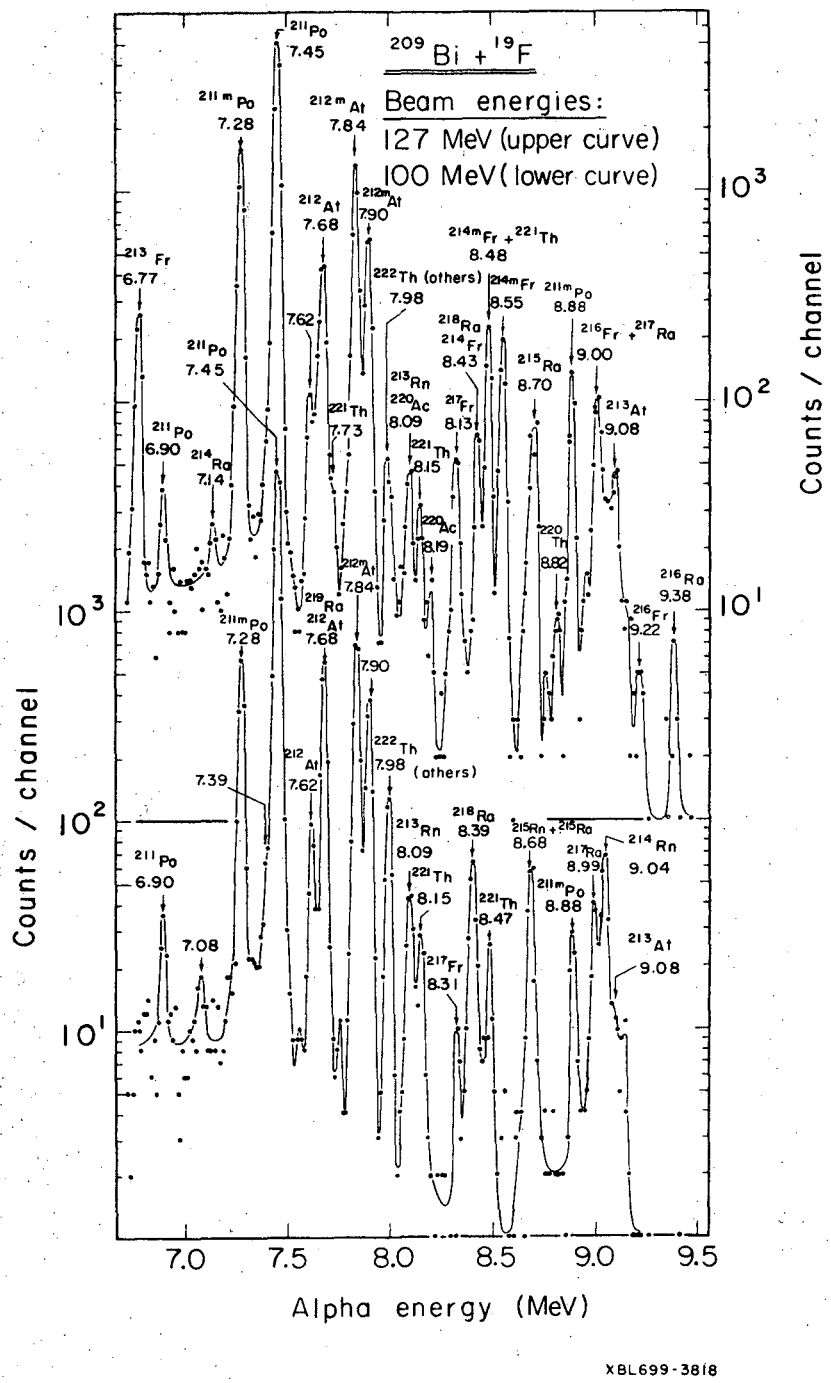
209 Bi + 19 F
Beam energies:
127 MeV (upper curve)
100 MeV (lower curve)
Counts / channel
Alpha energy (MeV)
XBL699-3818

Fig. 8

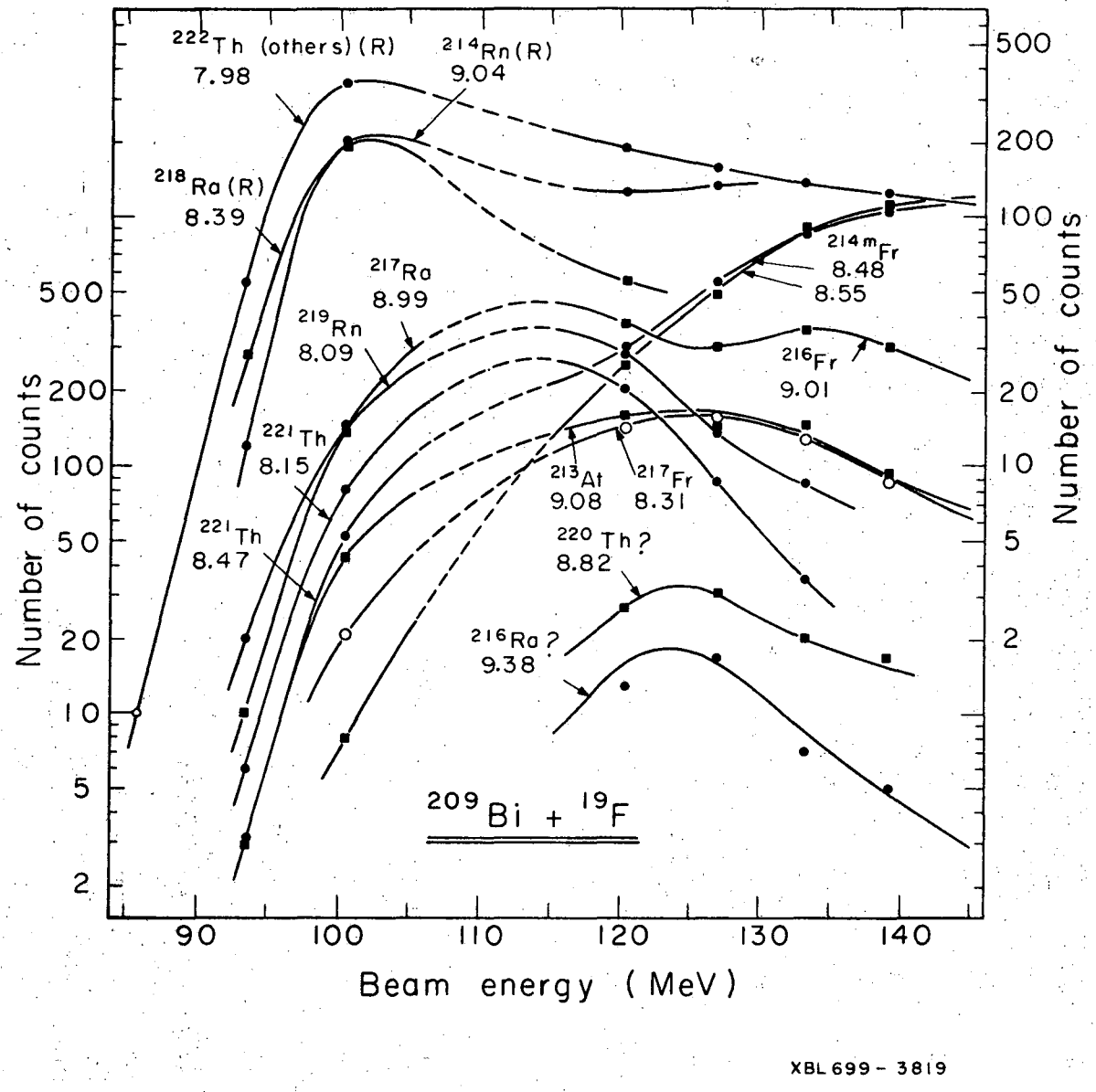

XBL 699 - 3819

Fig. 9

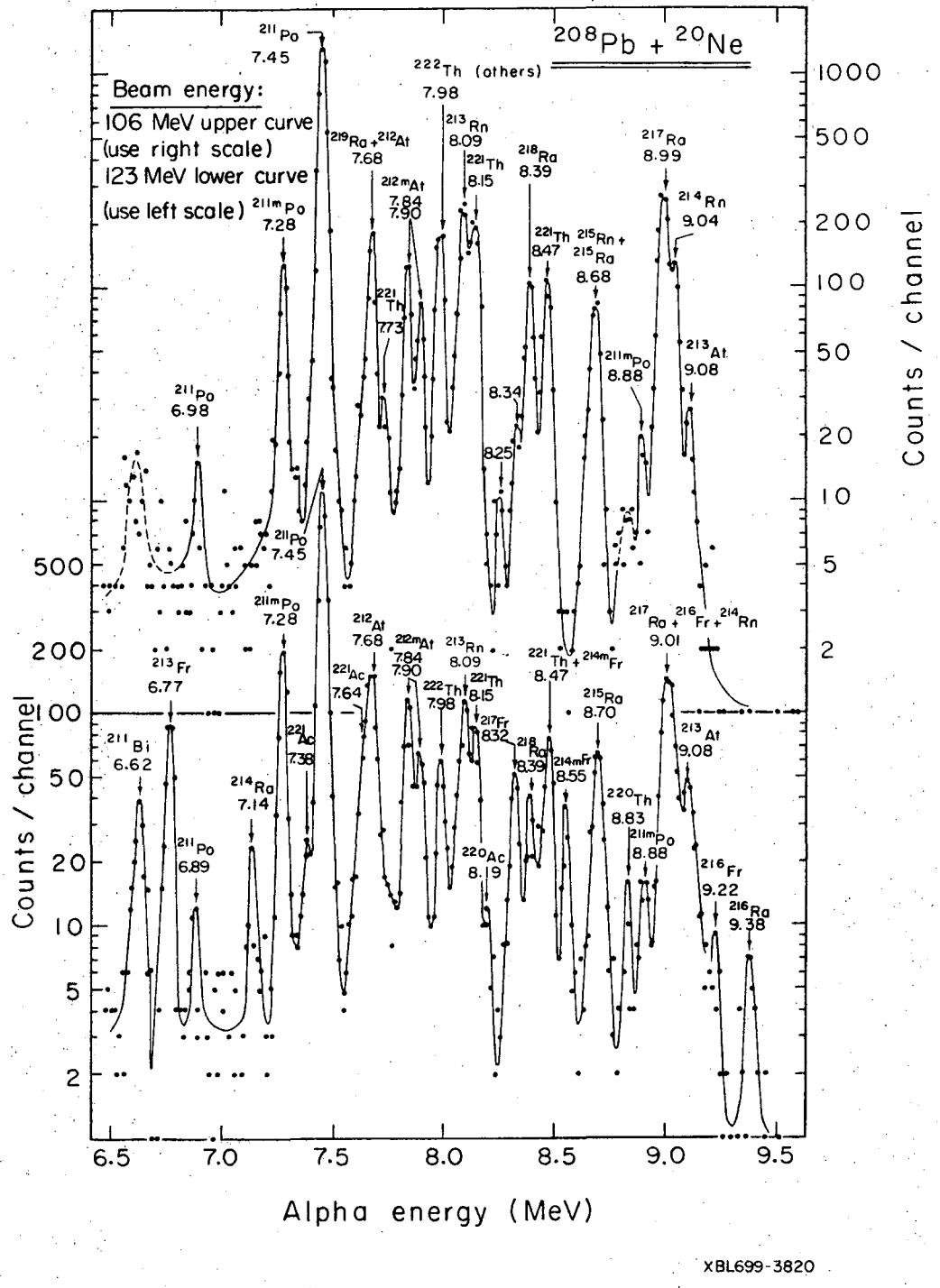
208Pb + 20Ne
Beam energy:
106 MeV upper curve
(use right scale)
123 MeV lower curve
(use left scale)
Counts / channel
Alpha energy (MeV)
XBL699-3820

Fig. 10

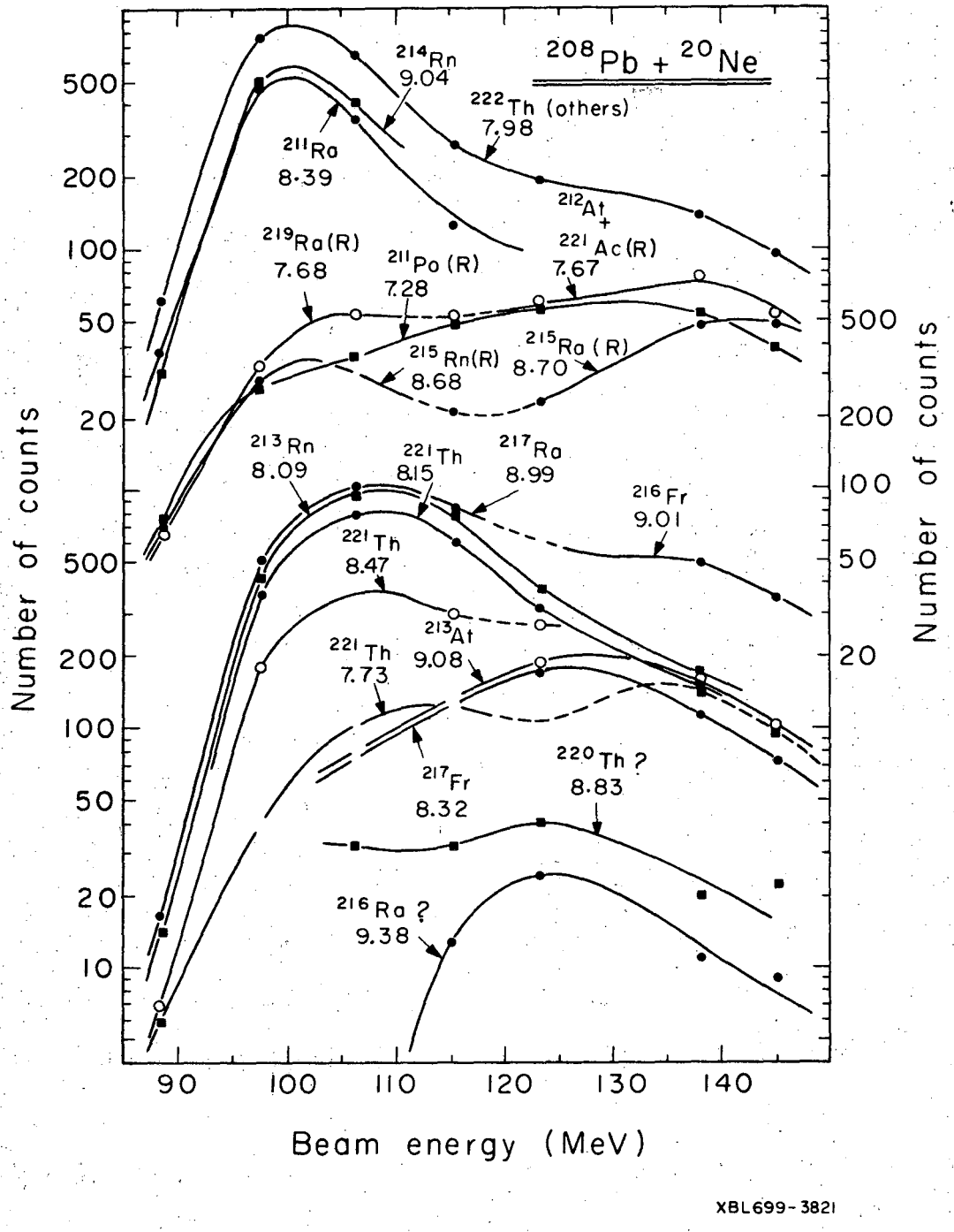
208Pb + 20Ne
214Rn 9.04
222Th (others) 7.98
211Ra 8.39
212At
219Ra(R) 7.68
211Po (R) 7.28
221Ac(R) 7.67
215Rn(R) 8.68
215Ra (R) 8.70
213Rn 8.09
221Th 8.15
217Ra 8.99
216Fr 9.01
221Th 8.47
213At 9.08
221Th 7.73
217Fr 8.32
220Th ? 8.83
216Ra ? 9.38
Number of counts
Number of counts
Beam energy (MeV)
XBL699-3821

Fig. 11

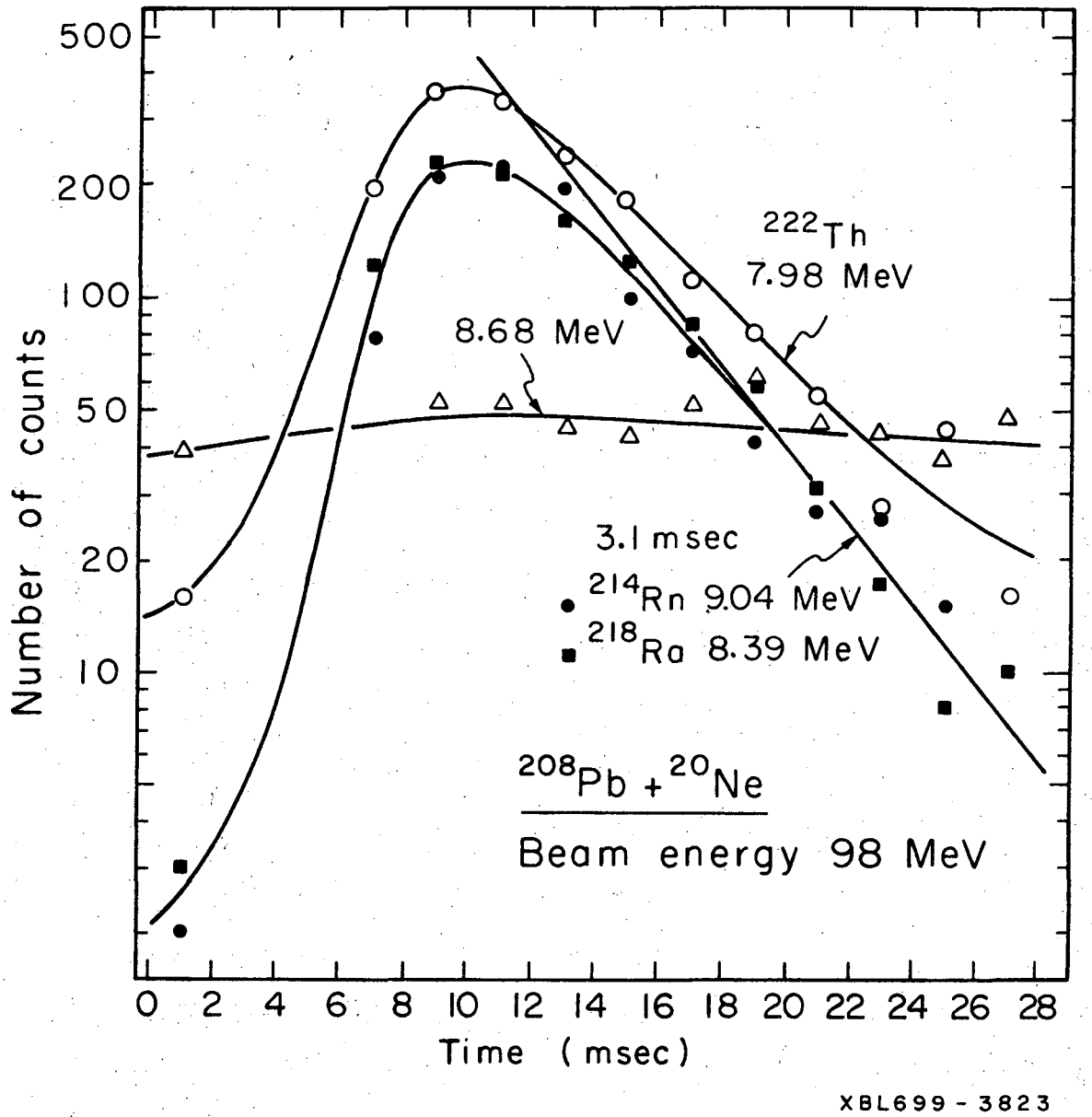
500
200
100
50
20
10
Number of counts
0 2 4 6 8 10 12 14 16 18 20 22 24 26 28
Time (msec)
222Th
7.98 MeV
8.68 MeV
3.1 msec
214Rn 9.04 MeV
218Ra 8.39 MeV
208Pb + 20Ne
Beam energy 98 MeV
XBL699-3823

Fig. 12

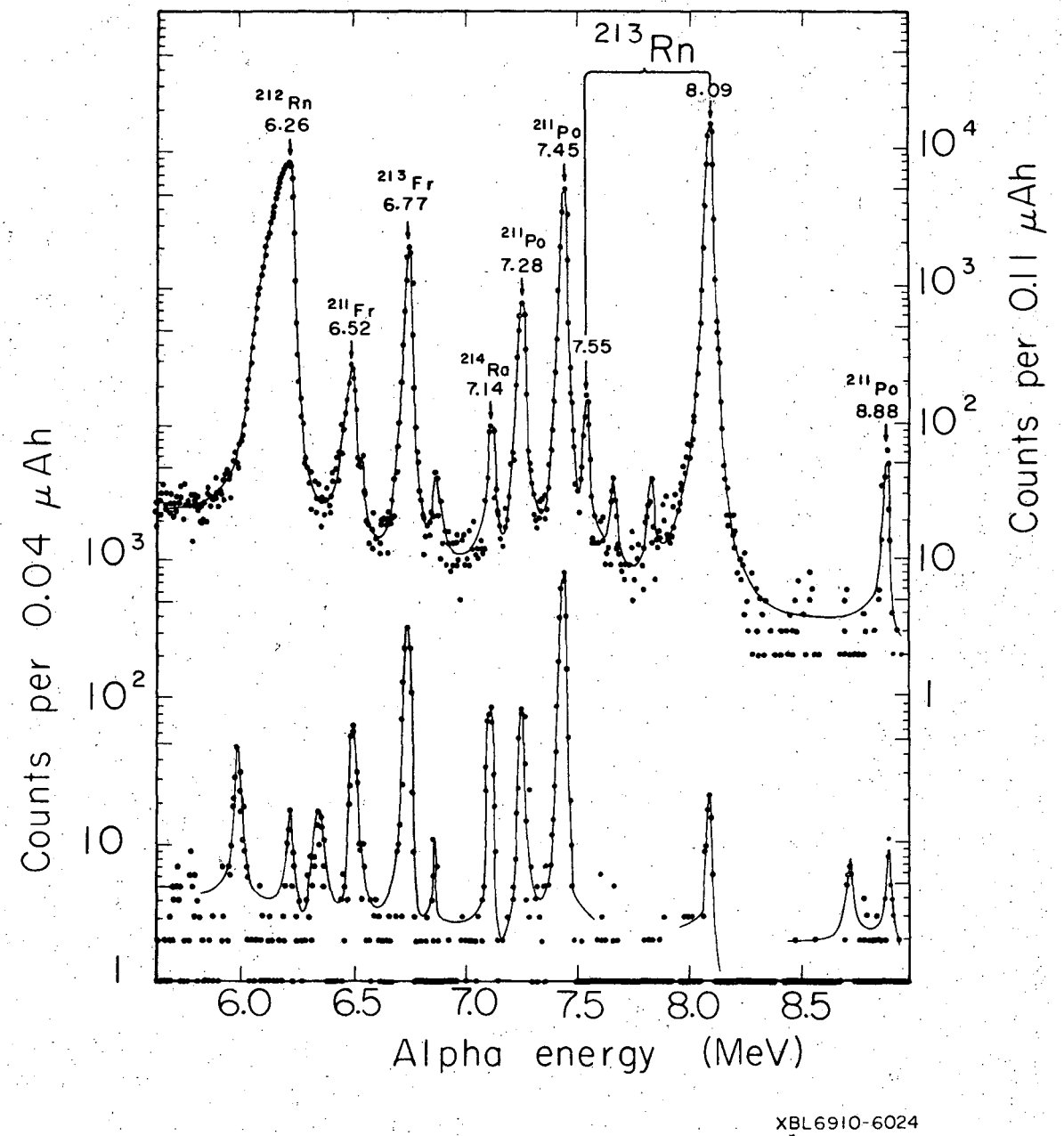
213 Rn
8.09
212 Rn
6.26
213 Fr
6.77
211 Po
7.45
211 Po
7.28
211 Fr
6.52
214 Ra
7.14
7.55
211 Po
8.88
Counts per 0.04 μAh
Counts per 0.11 μAh
10 4
10 3
10 2
10
1
10 3
10 2
10
1
6.0
6.5
7.0
7.5
8.0
8.5
Alpha energy (MeV)
XBL6910-6024

Fig. 13

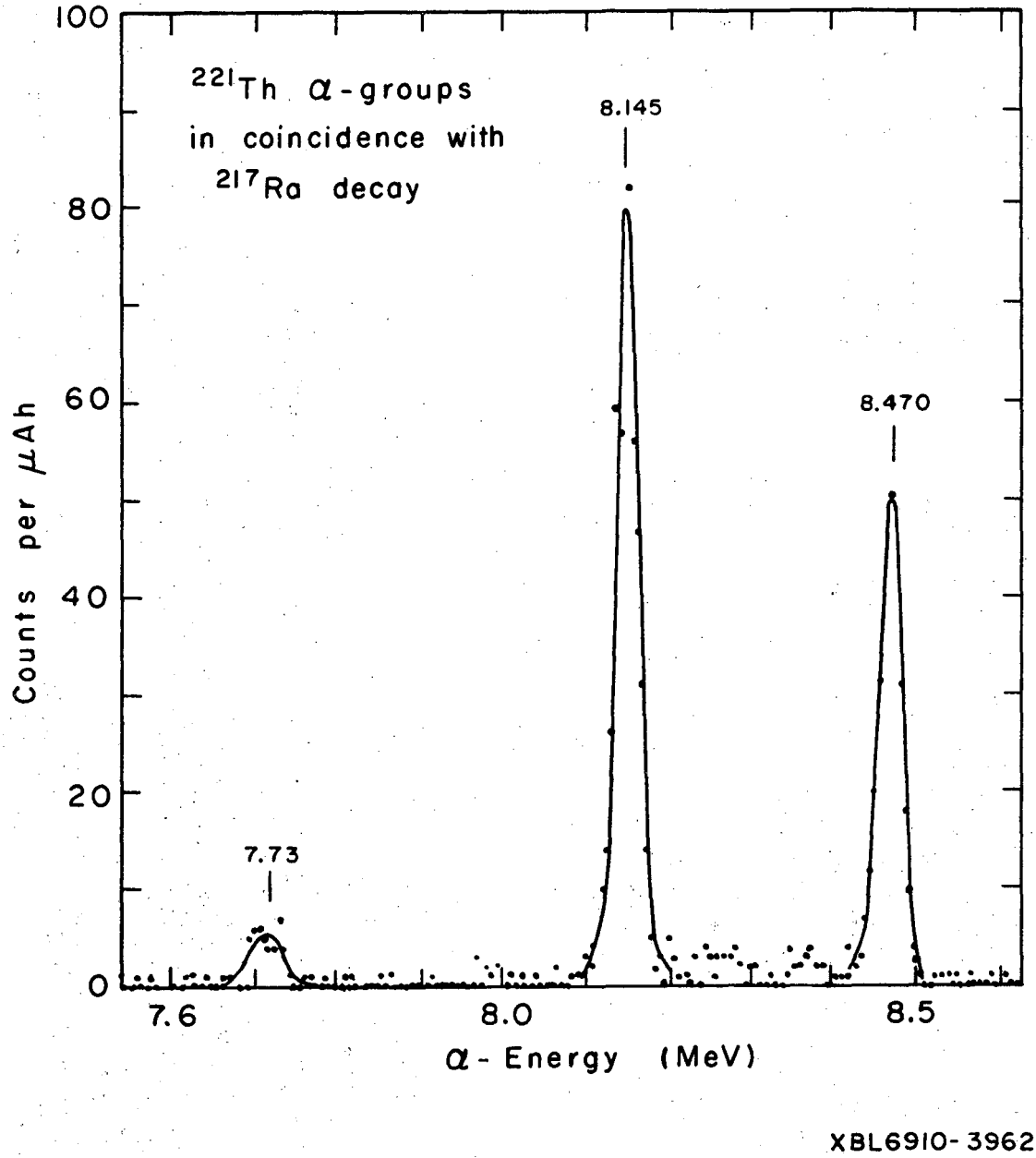
^{221}Th α-groups
in coincidence with
^{217}Ra decay
8.145
8.470
7.73
Counts per μAh
100
80
60
40
20
0
7.6
8.0
8.5
α - Energy (MeV)
XBL6910-3962

Fig. 14

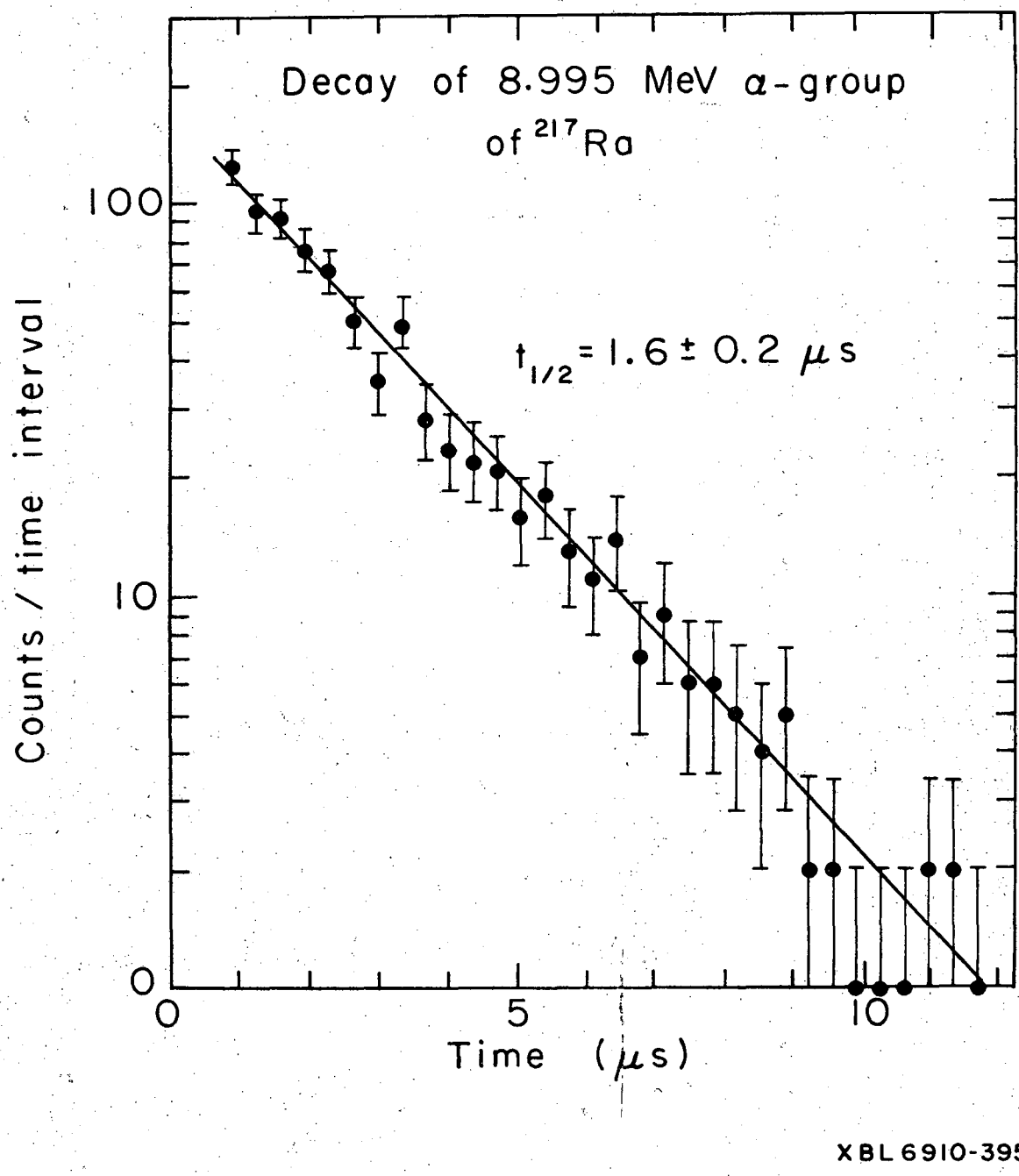
Decay of 8.995 MeV α-group
of ^{217}Ra
$t_{1/2} = 1.6 \pm 0.2$ μs
Counts / time interval
100
10
0
0
5
10
Time (μs)
XBL 6910-3951

Fig. 15

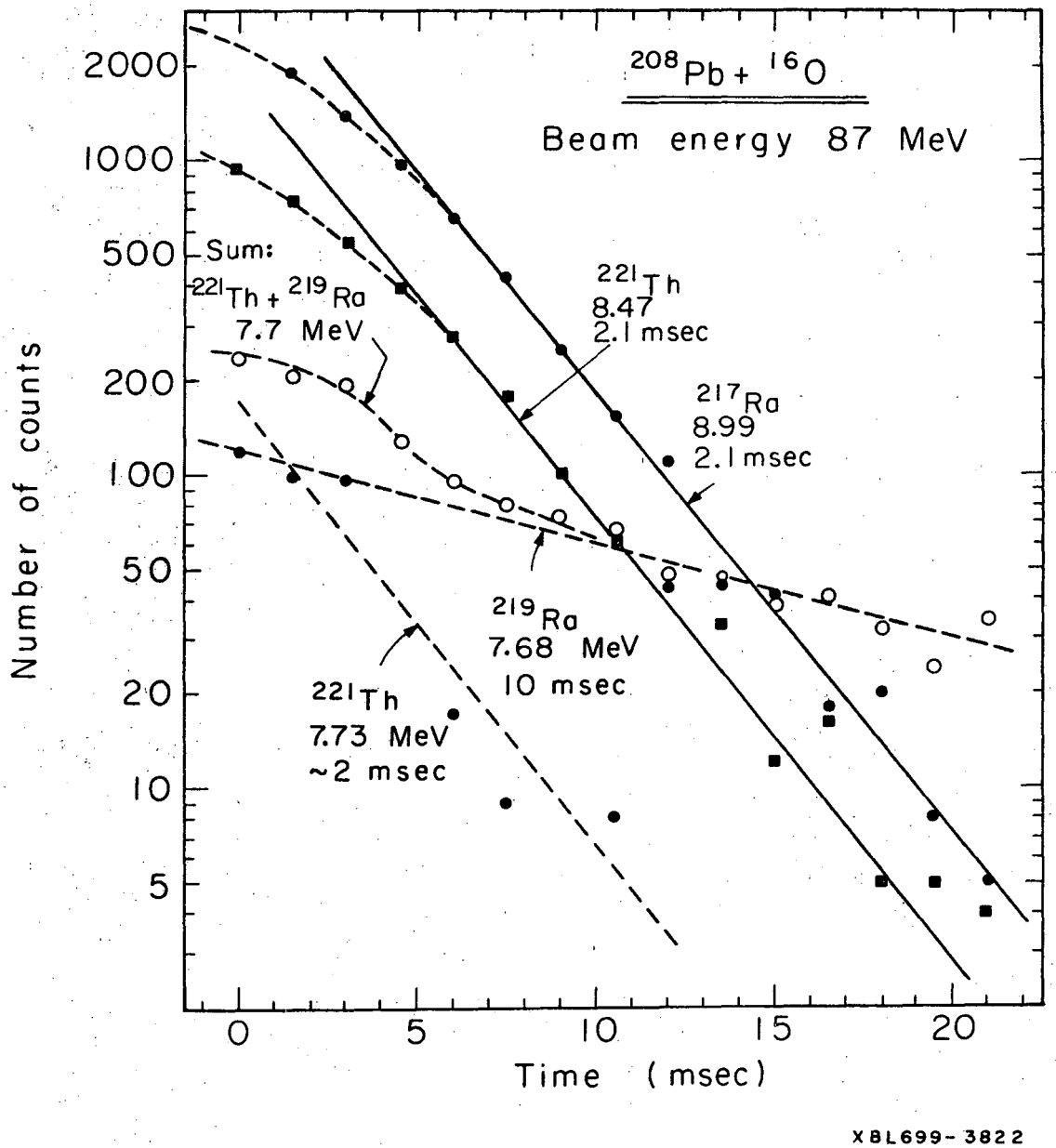
$^{208}Pb + ^{16}O$
Beam energy 87 MeV
Sum:
$^{221}Th + ^{219}Ra$
7.7 MeV
^{221}Th
8.47
2.1 msec
^{217}Ra
8.99
2.1 msec
^{219}Ra
7.68 MeV
10 msec
^{221}Th
7.73 MeV
~2 msec
Number of counts
Time (msec)
2000
1000
500
200
100
50
20
10
5
0
5
10
15
20
XBL699-3822

Fig. 16

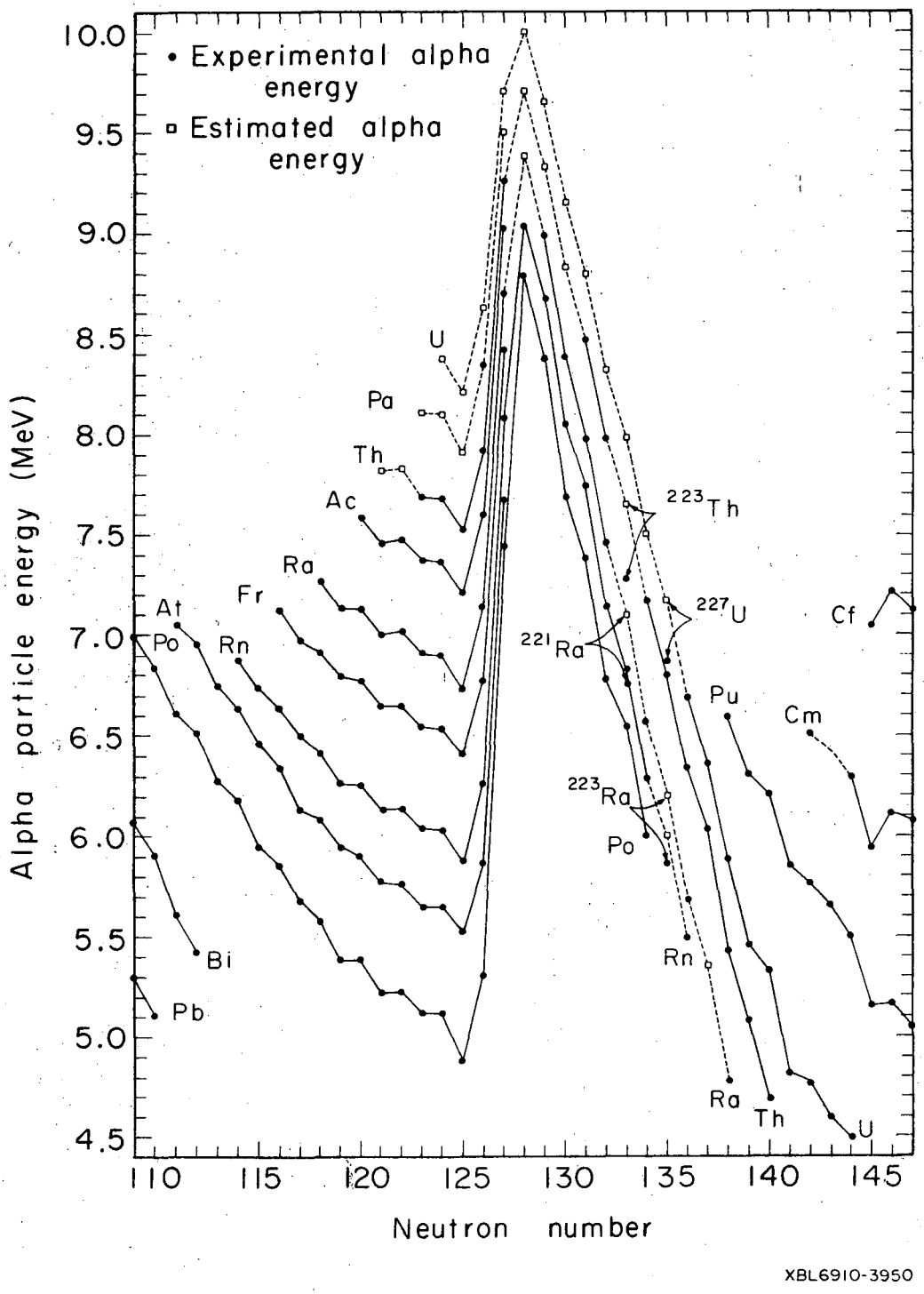
• Experimental alpha energy
▫ Estimated alpha energy
Alpha particle energy (MeV)
Neutron number
10.0
9.5
9.0
8.5
8.0
7.5
7.0
6.5
6.0
5.5
5.0
4.5
110
115
120
125
130
135
140
145
U
Pa
Th
Ac
Ra
Fr
At
Po
Rn
Bi
Pb
223Th
227U
221Ra
223Ra
Po
Rn
Ra
Th
U
Pu
Cm
Cf
XBL6910-3950

Fig. 17

LEGAL NOTICE

TECHNICAL INFORMATION DIVISION
LAWRENCE RADIATION LABORATORY
UNIVERSITY OF CALIFORNIA
BERKELEY, CALIFORNIA 94720